DOI: 10.1002/chem.201302327

Chiral Ditopic Cyclophosphazane (CycloP) Ligands: Synthesis, Coordination Chemistry, and Application in Asymmetric Catalysis

Torsten Roth,[a] Hubert Wadepohl,[a] Dominic S. Wright,*[b] and Lutz H. Gade*[a]

Dedicated to Professor Brian F. G. Johnson on the occasion of his 75th birthday

Abstract: A series of dichlorocyclophosphazanes [{ClP(μ-NR)}$_2$] containing chiral and achiral R groups was obtained from simple commercially available amines and PCl_3. Their condensation reactions with axially chiral biaryl diols yielded *ansa*-bridged chiral cyclophosphazane (CycloP) ligands. This highly modular methodology allows extensive elaboration of the ligand set, in which the chirality can be introduced at the diol bridge and/or the amido R group. This provides the possibility to observe match and mismatch effects in catalysis. A series of twenty CycloP ligands was synthesized and characterized by multinuclear NMR spectroscopy, HRMS, elemental analysis, and in selected cases, single-crystal X-ray diffraction. These studies show that all of the ditopic CycloP ligands are C_2 symmetric, rendering their metal coordination sites symmetry equivalent. Two well-established enantioselective reactions were explored by using late-transition metal CycloP complexes as catalysts; the gold-catalyzed hydroamination of γ-allenyl sulfonamides and the asymmetric nickel-catalyzed three-component coupling of a diene and an aldehyde. The steric demands of the CycloP ligands have a subtle influence on the reactivity and selectivity observed in both reactions. Good enantiomeric ratios (e.r.) as high as 89:11 in the gold-catalyzed reaction and 92:8 in the nickel-catalyzed bis-homoallylation reaction were observed.

Keywords: asymmetric catalysis · chiral ligands · phosphazanes · synthetic methods · X-ray diffraction

Introduction

Chiral phosphorus compounds occupy a pivotal role as ligands and precursors for a variety of transformations and are ubiquitous in a broad range of industrial and academic asymmetric catalytic reactions.[1] Early examples of chiral phosphorus ligands introduced by Knowles et al.[2] and Horner et al.[3] were monodentate, however, these were rapidly superseded by C_2-symmetric bidentate ligands introduced by Kagan et al.[4] More than two decades later Alexakis et al.,[5] Feringa et al.,[6] Reetz et al.,[7] and Pringle et al.[8] successfully challenged the conventional wisdom of the superior enantioselectivity of bidentate chiral catalysts by introducing monodentate phosphordiamide, phosphoramidite, phosphite, and phosphonite ligands (Figure 1), which gave comparable enantioselectivities to the established C_2-symmetric bidentate counterparts. The main advantages of these ligand scaffolds compared to previously existing arrangements of chiral aryl and alkyl phosphines is their robustness as well as the ease by which they can be prepared and their steric and electronic demands elaborated.[9]

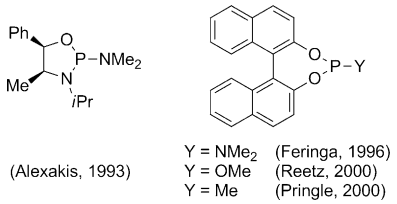

Figure 1. Monodentate phosphoramidite, phosphite, and phosphonite ligands.

The modular construction of ligands of this type enables chirality to be introduced either through the chelating component, the amine substituent, or both. Modification of the chirality of both components provides the potential for diastereomeric ligand pairs. A conspicuous feature of the very successful phosphoramidite and phosphite ligands is their reliance on their axially-chiral, rigid diol fragments as the source of chirality and conformational constraint. Besides the ubiquitous binol unit, taddol, vanol, and spinol have also proven to be "privileged" groups in numerous transformations in recent years.[10]

In 1977, Thompson and Keat reported that the reaction of dichlorophosphazanes with diols and diamines gives transan-

[a] Dipl.-Chem. T. Roth, Prof. Dr. H. Wadepohl, Prof. Dr. L. H. Gade
Anorganisch Chemisches Institut, Universität Heidelberg
Im Neuenheimer Feld 270, 69120 Heidelberg (Germany)
Fax: (+49) 6221-54-5609
E-mail: lutz.gade@uni-hd.de

[b] Prof. Dr. D. S. Wright
Chemistry Department, Cambridge University
Lensfield Rd, Cambridge CB2 1EW (UK)
Fax: (+44) 1223-336362
E-mail: dsw1000@cam.ac.uk

Supporting information for this article is available on the WWW under http://dx.doi.org/10.1002/chem.201302327.

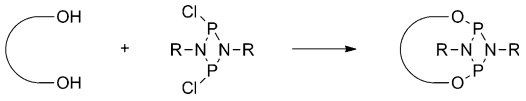

Scheme 1. Synthesis of diol-bridged cyclophosphazanes by Thompson and Keat.[11]

nular bicyclic phosphazanes in which the normal tendency for *cis–trans*-isomerization and dissociation of the P_2N_2 ring unit is suppressed (see Scheme 1).[11]

More recently, by using the same methodology, Swamy et al. prepared several biaryl-bridged representatives of this class of cyclophosphazanes[12] (Figure 2, **I**) and the first

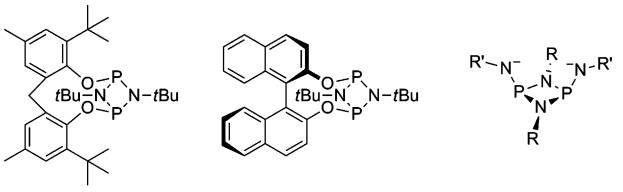

Figure 2. Achiral and chiral bridged cyclophosphazanes **I** and **II** as synthesized by Swamy et al. and dianionic bis(amido)cyclodiphosphazanes **III**.

chiral representatives by employing a binol backbone (Figure 2, **II**).[13] However, despite being structurally and electronically closely related to the phosphoramidites, the bidentate cyclophosph(III)azanes have so far found only limited use in catalysis and there are no examples of asymmetric catalysis involving this type of ligand framework.[14] A noteworthy exception are the dianionic chelating bis(amido)cyclodiphosphazanes, $[\{(RN)P(\mu\text{-}NR)\}_2]^{2-}$ (Figure 2, **III**) that were reported by Stahl and Chivers et al.,[15] which have recently garnered attention as ligands for Group 4-based olefin polymerization catalysts.[16]

Chiral cyclophosphazane (CycloP) ligands like **II** in Figure 2 have several unique and important characteristics, which are in stark contrast to more conventional ligands used in catalysis. In particular they have a convex ligand topology and an exodentate spatial arrangement of the phosphorus lone pairs making them potentially ditopic ligands. Importantly, with regard to their application as stereo-directing ligands in catalysis, the cyclophosphazane framework should be remarkably easily elaborated by a series of modular reactions both at the bridging amido groups within the P_2N_2 units and at the transannular bridge. Similar to the ligand systems shown in Figure 1, there is also the possibility of introducing chirality at either of these key positions, that is, introducing the potential for matched and mismatched pairs. In view of the bis-monodentate character of CycloP ligands, that is, coordination of two metal centers rather than it acting as a chelate ligand[17] there is also a unique potential for cooperative activation by using both metal centers,[18] as commonly utilized in enzyme biocatalysis.[19]

Following our recent work on the investigation of the influence of multiple metal centers on the enantioselectivity of gold-catalyzed transformations,[20] we became interested in the cyclophosphazane moiety, its dimetallic complexes, and its potential for cooperative interactions in catalytic reactions. In the current paper we show that 1) a very large number of CycloP ligands of the type **II** can be easily accessed, which are chiral at the transannular bridge or (for the first time) at the amido group or both, 2) these ligands coordinate catalytically active late-transition metals such as rhodium, copper, iridium, gold, and nickel, and 3) the metal complexes of the CycloP ligands can be employed as catalysts for asymmetric transformations with good enantioselectivity.

Results and Discussion

Synthesis and characterization of chiral cyclophosphazane (CycloP) ligands

Synthesis and characterization of dichlorocyclophosphazane precursors: The first step in the systematic elaboration of chiral cyclophosphazanes was to synthesize a range of new dichlorodimers of the type $[\{ClP(\mu\text{-}NR)\}_2]$. Previously, only a limited number of dimers of this type had been structurally characterized.[21] One of the primary aims of the initial synthetic studies was to broaden the range of the available dimers, which could be used as precursors for the synthesis of the CycloP ligands described in the next section. A further aim was to synthesize the first dichlorophosphazane dimers containing chiral groups within the R–N substituent. This was thought to be a key element in the formation of new CycloP scaffolds having chirality both at the bridge and the R–N group, hence the potential for match and mismatch ligand effects.

Initially, a range of synthetic approaches for the formation of dichlorocyclophosphazanedimers was evaluated, based on known literature procedures. It quickly became apparent that the best approach to these species using a broad range of organic substituents was the condensation of PCl_3 with primary amines in the presence of excess triethylamine as the Brønsted base (Scheme 2).

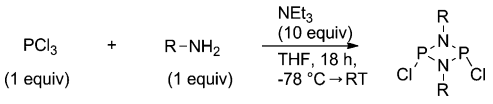

Scheme 2. General synthesis of dichlorocyclophosphazanes.

The organic substituents (R) were selected based on their steric demands. The use of bulky substituents ensured the retention of the P_2N_2 ring units because it is known from previous studies that small substituents (such as R = Me, Et) could result in the formation of higher cyclic oligomers or cages.[22]

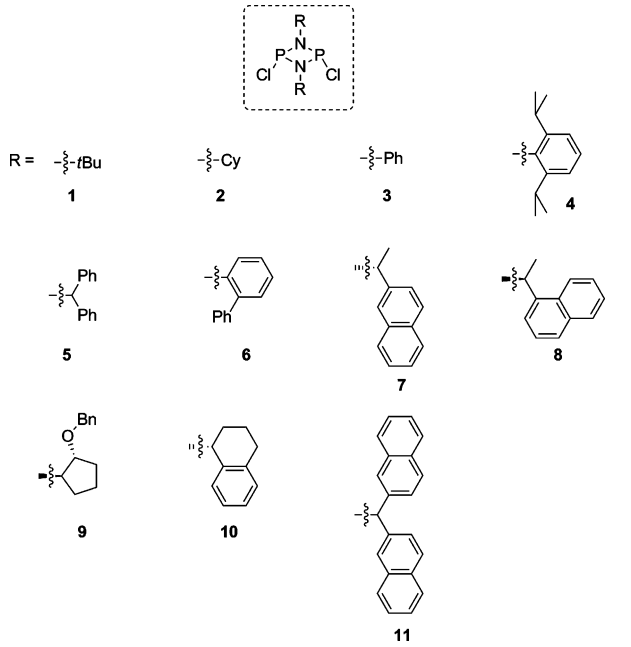

Figure 3. Numbering scheme for the *N*-alkylated and *N*-arylated cyclophosphazanes. Numbers correspond to the $P_2(NR)_2$ fragment.

The previously reported compounds **1**·Cl_2–**4**·Cl_2 (R = *t*Bu (**1**), cyclohexyl (Cy, **2**), Ph (**3**), 2,6-diisopropylphenyl (dipp, **4**)) were prepared according to literature procedures, whereas the new P_2N_2 dimers **5**·Cl_2–**11**·Cl_2 were obtained in moderate yields by the condensation reaction shown in Scheme 2 (see Figure 3 for the numbering scheme used in the text). Importantly, the products could be prepared on a multigram scale by this procedure. In addition to ^{31}P and ^{1}H NMR spectroscopy, all of the new compounds **5**·Cl_2–**11**·Cl_2 were characterized by a combination of LIFDI(+) mass spectrometry, elemental analysis, and, in the case of **6**·Cl_2, by single-crystal X-ray diffraction. For all of the compounds the LIFDI(+) mass spectra in toluene gave a highest molecular ion peak corresponding to $[M]^+$, thus indicating, that the dimeric structures were maintained in the gas phase. Particularly diagnostic is the ^{31}P NMR spectroscopic shift of dimers **1**·Cl_2–**11**·Cl_2, which was found in the range $\delta = 200$ to 225 ppm. This chemical shift range is typical of dimeric *cis*-P_2N_2 units and can be compared to dimers in which the chloride substituents are *trans* to the P_2N_2 plane (shifted by $\delta = 80$–90 ppm to lower field compared to the *cis* dimer).[23] It is known that for relatively sterically unencumbered substituents R, which have low electronegativity, the *cis* structure is marginally more stable in solution and in the gas phase.[23] The dichlorocyclophosphazane **9**·Cl_2 is noteworthy in being a rare example of a P_2N_2 dimer containing donor-functionalized R groups that can potentially coordinate metal centers.[24]

The solid-state molecular structure of dimer **6**·Cl_2, which was a key precursor in later studies is shown in Figure 4. The plane of the *N*-bonded aryl substituent is skewed by approximately 50° out of the plane of the P_2N_2 ring.

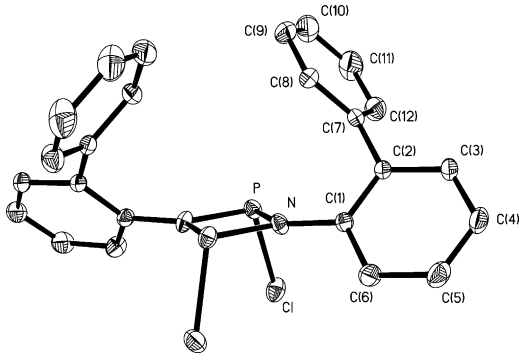

Figure 4. Molecular structure of compound **6**·Cl_2, thermal ellipsoids set at the 50% probability level. Hydrogen atoms are omitted for clarity. Selected bond lengths [Å] and angles [°]: P–Cl 2.1276(4), P′–N 1.6983(10), P–N 1.7137(9); P′-N-P 99.09(5), N′-P-N 80.90(5), P-N-C(1)-C(6) 133.3(1).

Chiral cyclophosphazane ligands: The next step was to obtain the CycloP ligands by incorporating a chiral backbone. These ligands were prepared by using the condensation reactions of the dichlorphosphazanes **1**·Cl_2–**11**·Cl_2 with the bridging diols binol, vanol, and vapol in the presence of NEt_3 as the Brønsted base (Scheme 3).

Initially, we investigated the behavior of the bis(mentholate) phosphazane dimer **A** prepared by the reaction shown in Scheme 4. Its structural chemistry illustrates the level of

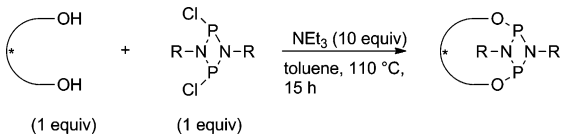

Scheme 3. General synthesis of bridged cyclophosphazane ligands.

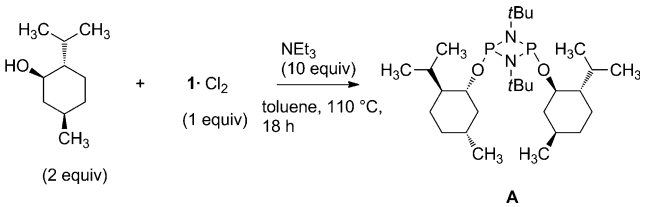

Scheme 4. Synthesis of the bis(mentholato) cyclophosphazane A.

complexity to be encountered when not using diols that give rise to the well-defined bicyclic structures discussed in detail below.

The molecular structure of **A** determined by X-ray diffraction shows a *cis* arrangement of the menthol groups with respect to the P_2N_2 ring. In addition, the menthol rings themselves adopt *exo* and *endo* orientations with respect to the P_2N_2 ring unit (Figure 5). Such *exo*/*endo* orientation of N(–H)- and O-bonded substituents has been seen previously in the solid-state structures of cyclophosphazane macrocycles.[25] As for these macrocycles a variable-temperature (VT) ^{31}P NMR study revealed that rapid *exo*/*endo* inversion

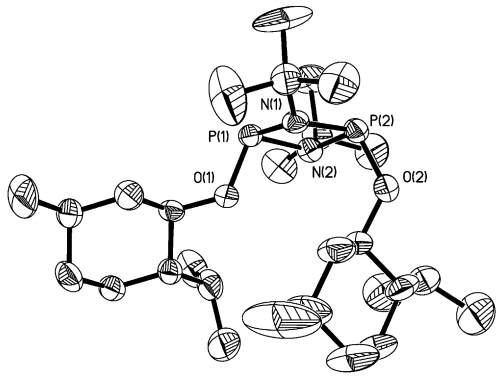

Figure 5. Molecular structure of compound **A**. The menthol moiety on O(1) adopts an *endo* and the menthol group on O(2) an *exo* orientation.[25a] Thermal ellipsoids set at the 50% probability level. Hydrogen atoms are omitted for clarity. Selected bond lengths [Å] and angles [°]: P(1)–O(1) 1.626(4), P(2)–O(2) 1.622(5), P–N 1.713(5)…1.737(5); P(1)-N(2)-P(2) 96.7(2), N(1)-P(1)-N(2) 82.4(2), O(1)-P(1)-P(2)-O(2) 2.2(3).

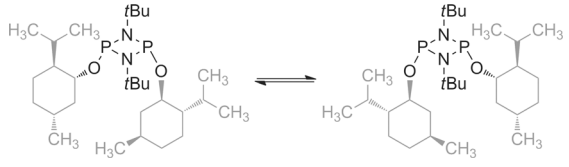

Scheme 5. Fluxional behavior of bis(mentholato) cyclophosphazane **A** in solution.

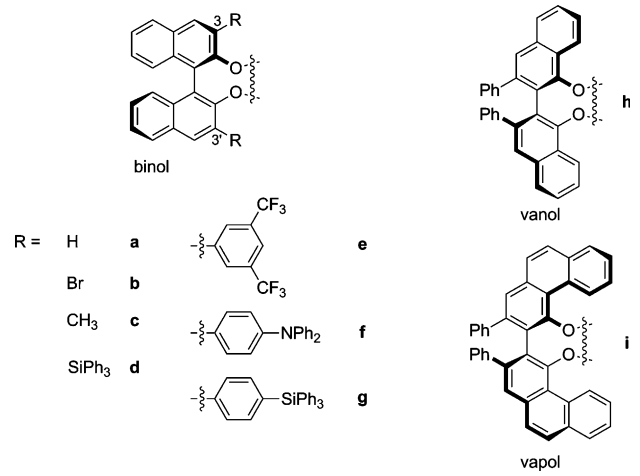

Figure 6. Numbering scheme for chiral diol bridging groups. Letters correspond to the diaryloxy fragment.

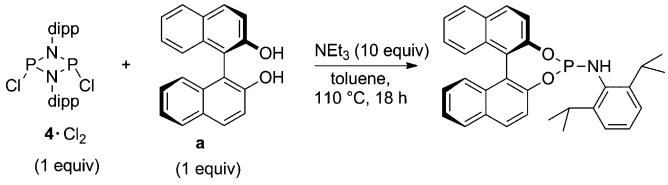

Scheme 6. Observed fragmentation–condensation reaction of dichlorocyclophosphazane **4**·Cl_2.

of the oxygen atoms occurs at room temperature (Scheme 5).

The corresponding free energy of activation ($\Delta G^{\neq}$) for this process of 31 kJ mol^{-1} was found to be similar to that previously reported for oxygen-bridged phosphazane macrocycles.[25b]

The significance of the fluxionality of **A** is that ligand systems involving separate and disconnected chiral groups bonded to phosphorus are unlikely to be efficient ligands for asymmetric metal catalysis because the steric domain of the coordination environment on either side of the ligand does not remain static. In contrast, *ansa*-bridged chiral CycloP ligands should not suffer from this problem. Following the general procedure depicted in Scheme 3, we prepared the binol derivative **1a**[12a] (72% yield) and the vanol-bridged ligand **1h** (59% yield) (see Figures 3 and 6 for the numbering scheme used throughout this work).

The retention of the P_2N_2 ring unit and the formation of the desired chiral bridged cyclophosphazane proved to be critically dependent on the steric bulk of the amido group R–N and of the bridging framework. In general, it is notable, that the sterically less demanding combinations of diol and dichlorophosphazane resulted in cleaner product formation, whereas the bulkier derivatives had to be further purified by column chromatography. An extreme case of this was observed in the reaction of the sterically encumbered compound **4**·Cl_2 with unsubstituted binol **a**, which gives rise to disruption of the P_2N_2 ring and formation of the corresponding phosphoramidite as suggested by NMR spectroscopy (Scheme 6). In addition, the reaction of sterically demanding vapol **i** with **1**·Cl_2 only yielded an intractable mixture of products.

We therefore decided to focus on the binol framework in all further studies. Whereas almost all of the binols **a**–**e** are commercially available, binols **f** and **g** are novel derivatives and were conveniently prepared by Suzuki coupling reactions (see the Supporting Information). Our thinking in regard to these ligand frameworks was that steric and electronic modification at the 3,3′-positions would have the greatest impact on the metal-coordinating phosphorus donor site. Most importantly 3,3′-substitution of the binol core provided the maximum possible transmission of chirality to the phosphorus site. This "long-arm effect" had recently been exploited in binol and spinol phosphoramidites.[26]

Figure 7 lists all of the new CycloP ligands, which were prepared in this study. All products obtained are colorless solids and remarkably air stable, for example, air exposure of **1a** for several days resulted in only partial decomposition, typically giving a yellow discoloration. The new CycloP ligands were characterized by a combination of HRMS (FAB(+)), multinuclear (^{1}H, ^{31}P, ^{13}C, ^{29}Si, ^{19}F) NMR spectroscopy, and elemental analysis., and in selected cases by single-crystal X-ray diffraction (compounds **1b**, **1c**, **2a**, **5a**, **6a**, and **7c**). All of the products listed in Figure 7 were characterized by a single singlet ^{31}P{^{1}H} NMR shift (generally

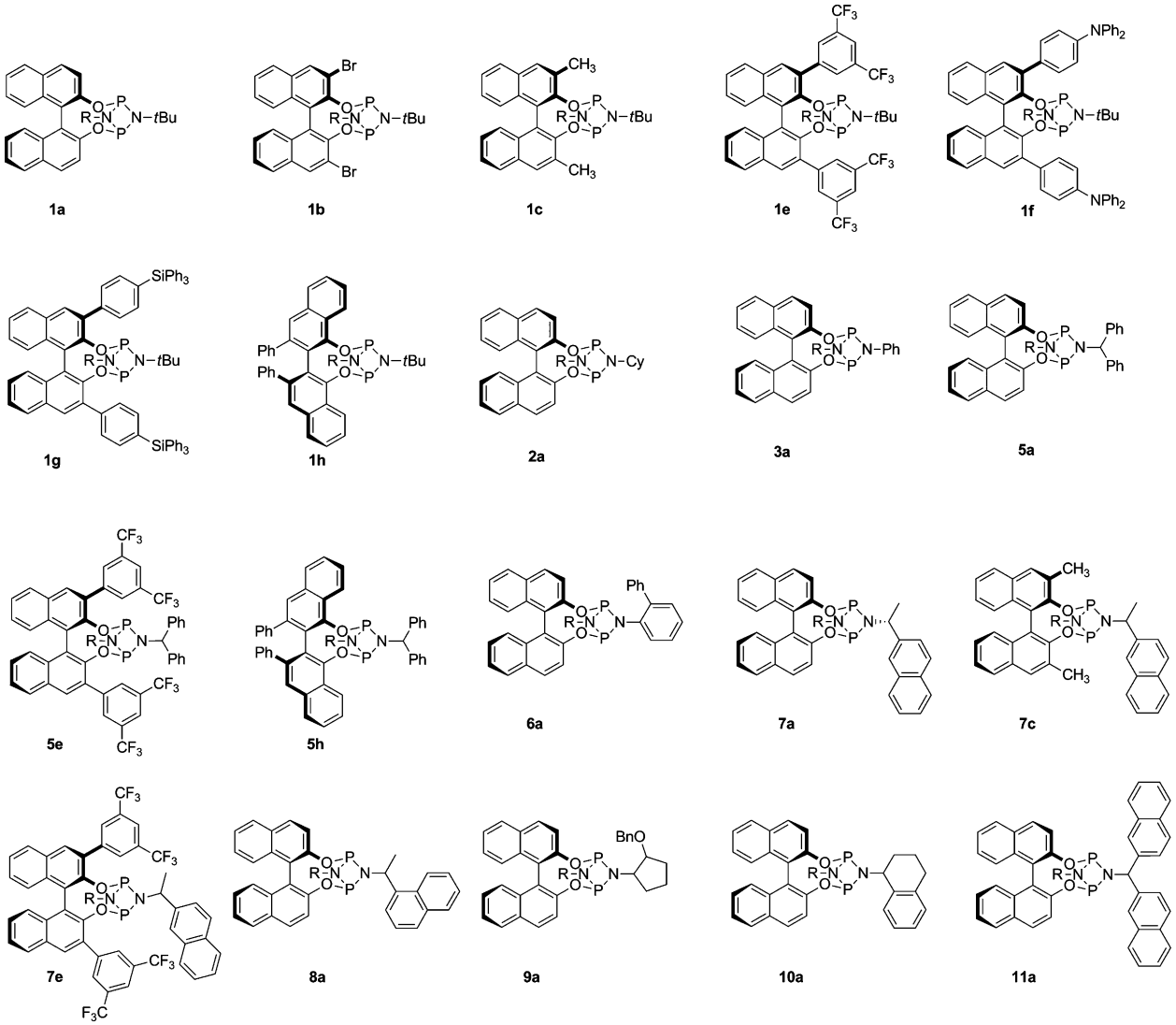

Figure 7. Complete list of the chiral cyclophosphazane ligands synthesized in this work. One amido R group is omitted for clarity.

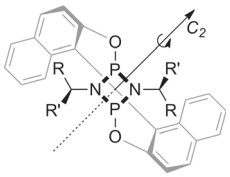

Figure 8. Illustration of the C_2 rotational axis in cyclophosphazane ligands containing chirality in the binol backbone and the amido substituent.

between $\delta = 164$ and 185 ppm), confirming, that the molecular C_2-symmetric axis is maintained in each case (Figure 8).

The main features of the new CycloP ligands were thus either chirality at the bridge only or both at the bridgehead and the amide group R. The latter allowed access to diastereomeric pairs and the probing of match/mismatch phenomena. These features are illustrated most clearly in the structurally characterized complexes **1b** (chiral at the bridge alone, Figure 9), and the diastereomers (R_{binol},R_{amine})-**10a** (Figure 10) and (S_{binol},R_{amine})-**10a** (Figure 11).

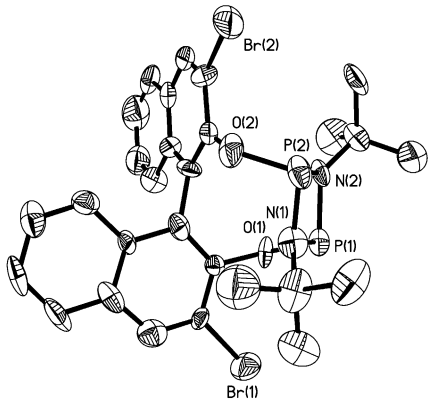

Figure 9. Molecular structure of compound (*R*)-**1b**, thermal ellipsoids set at the 50% probability level. Hydrogen atoms are omitted for clarity. Selected bond lengths [Å] and angles [°]: P(1)–N(1) 1.710(11), P(1)–O(1) 1.685(8); P(1)-N(1)-P(2) 97.6(6), N(1)-P(1)-N(2) 82.1(5).

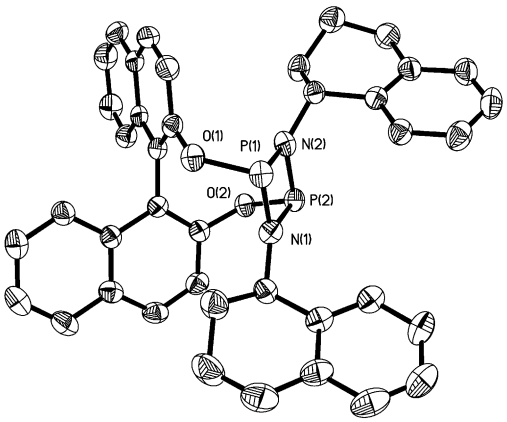

Figure 10. Molecular structure of compound (R_{binol},R_{amine})-**10a**, thermal ellipsoids set at the 50% probability level. One molecule of toluene and hydrogen atoms are omitted for clarity. Selected bond lengths [Å] and angles [°]: P(1)–N(1) 1.717(2), P(1)–O(1) 1.664(2); P(1)-N(1)-P(2) 98.5(1), N(1)-P(1)-N(2) 81.4(1).

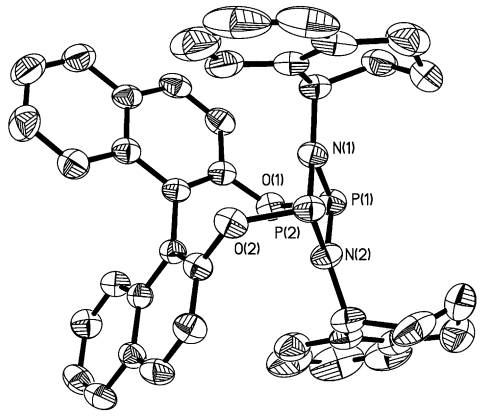

Figure 11. Molecular structure of compound (S_{binol},R_{amine})-dia-**10a**, thermal ellipsoids set at the 50% probability level. Hydrogen atoms are omitted for clarity. Selected bond lengths [Å] and angles [°]: P(1)–N(1) 1.704(2), P(1)–O(1) 1.667(2); N(1)-P(1)-N(2) 81.2(1), P(1)-N(1)-P(2) 98.6(1).

Coordination of chiral cyclophosphazanes to metals: In the next step of the study we investigated the complexation behavior of the two phosphorus lone pairs of the CycloP ligands to several late transition metals, in particular to assess the rigidity of the chiral ligands upon metal coordination. This was an important issue because previous studies suggested that *ansa* cyclophosphazanes of this type could potentially oligomerize giving dimeric macrocyclic species,[25b] and the presence of Lewis acidic metal centers could also result in ring-expansion.[27]

Moreover, the spatial arrangement around the catalytically active sites and any dynamic behavior at the metal centers were of interest. The coordination chemistry of achiral dimeric phosphazanes (related to the chiral system we report here) had been elaborated in great detail by several groups, resulting in a plethora of interesting mono- and oligo-metallic structures.[28] However, to the best of our knowledge, there were no previous reports of the coordination behavior of chiral phosphazane counterparts.

Initially, we investigated the reaction of ligand **1a** with the common gold(I) precursor [(Me_2S)AuCl] (1:2 equivalents) and found the transformation to the digold(I) complex was complete within 30 min at room temperature (Scheme 7). In situ $^{31}P\{^1H\}$ NMR spectroscopy showed that

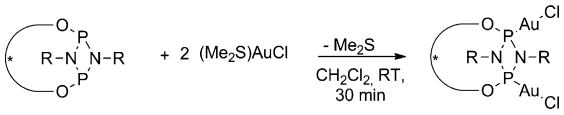

Scheme 7. General procedure for the synthesis of chiral digold(I)cyclophosphazane complexes.

the bis-coordination to two gold centers resulted in a decrease of the chemical shifts of the singlet resonance of approximately $\delta = 50$ ppm. Significantly, the ^1H and ^{31}P NMR spectra of [**1a**·$(AuCl)_2$] confirmed that the ligand remained intact in solution and that there was no rearrangement or oligomerization occurring upon metal coordination.

This was also confirmed by a single-crystal X-ray structure analysis of [**1a**·$(AuCl)_2$] (Figure 12). The structure reveals a

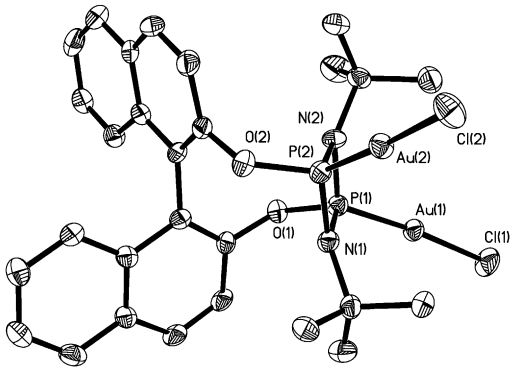

Figure 12. Molecular structure of compound (*R*)-[**1a**·$(AuCl)_2$], thermal ellipsoids set at the 50% probability level. Hydrogen atoms are omitted for clarity. Selected distances [Å], bond lengths [Å], and angles [°]: Au(1)···Au(2) 5.7321(2), P(1)–Au(1) 2.199(1), P(1)–N(1) 1.687(4), P(1)–O(1) 1.600(3); P(1)-Au(1)-Cl(1) 174.39(5), P(1)-N(1)-P(2) 94.8(2), N(1)-P(1)-N(2) 84.9(2).

very long intramolecular $Au^I \cdots Au^I$ distance of 5.7321(2) Å, which is well outside the range of aurophilic interactions.[29] This indicated that cooperativity between the two metal centers was unlikely in catalytic reactions.

A series of such gold(I) complexes containing CycloP ligands was prepared and fully characterized in the current work. The NMR spectroscopic characteristics of all of these complexes were similar to those discussed above for [**1a**·$(AuCl)_2$]. The single-crystal X-ray structure analysis of [**1a**·$(AuCl)_2$], [**1b**·$(AuCl)_2$], [**1c**·$(AuCl)_2$], [**1e**·$(AuCl)_2$], [**1g**·$(AuCl)_2$], [**1h**·$(AuCl)_2$] (Figure 13), and [**9a**·$(AuCl)_2$] were obtained (see the Supporting Information). Comparison of

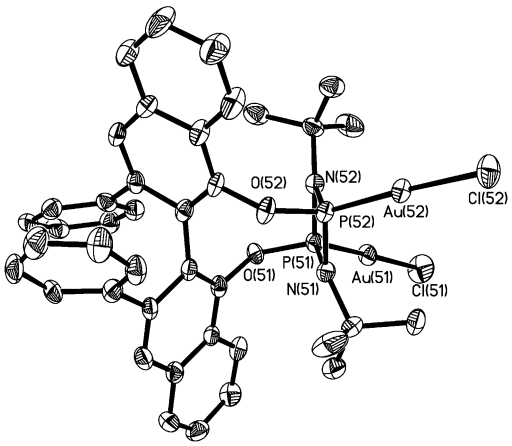

Figure 13. Molecular structure of compound [**1h**·$(AuCl)_2$], thermal ellipsoids set at the 50% probability level. Only one of the two independent molecules is shown. Hydrogen atoms are omitted for clarity. Selected bond lengths [Å] and angles [°]:P(51)–O(51) 1.601(5), P(51)–N(51) 1.678(6), P(51)–Au(51) 2.186(2), Au(51)–Cl(51) 2.257(2); P(51)-Au(51)-Cl(51) 176.89(9).

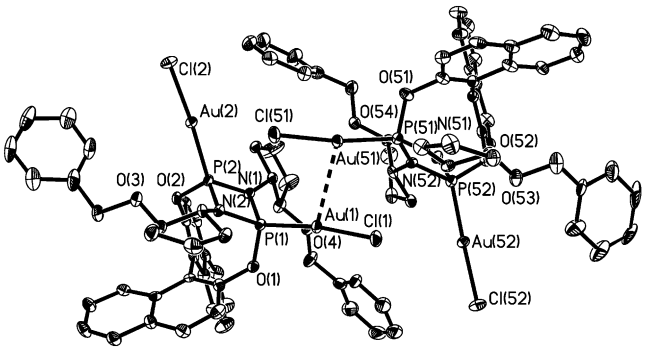

Figure 14. Molecular structure of dimeric compound [**9a**·$(AuCl)_2$], thermal ellipsoids set at the 50% probability level. The second set of the disordered OBn group and hydrogen atoms are omitted for clarity. Selected bond lengths [Å] and angles [°]: P(1)–Au(1) 2.205(2), P(2)–Au(2) 2.200(2), Au(1)–Au(51) 3.093(1), Au(1)–Cl(1) 2.282(2), Au(2)–Cl(2) 2.278(3); P(1)-Au(1)-Cl(1) 171.50(9), P(2)-Au(2)-Cl(2) 175.76(10), P(1)-Au(1)-Au(51)-P(51) 138.28(9).

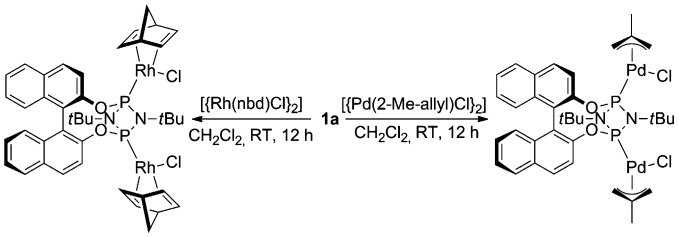

Scheme 8. Reaction of **1a** with the dimeric precursors [{Rh(nbd)$Cl\}_2$] (left) and [{Pd(2-Me-allyl)$Cl\}_2$] (right).

the $Au^I\cdots Au^I$ distances in the series of CycloP complexes [**1a**·$(AuCl)_2$], [**1b**·$(AuCl)_2$], [**1c**·$(AuCl)_2$], [**1e**·$(AuCl)_2$], and [**1g**·$(AuCl)_2$], in which there is increasing steric bulk of the 3,3′ substituents within the binol bridge, revealed that there is no resulting reduction in the metal···metal distance (≈5.71–5.98 Å). Interestingly, the 3,3′-aryl-substituted complexes [**1e**·$(AuCl)_2$] and [**1g**·$(AuCl)_2$] feature relatively short intramolecular $\pi_{aryl}\cdots Au^I$ distances of approximately 3.65 Å. Such short π-cation distances may exert significant stabilizing effects on catalytically active metal centers, an advantage exploited in the Buchwald ligand family.[1d,30]

A comprehensive discussion of all of the structurally characterized complexes is not provided here, however, the two complexes [**1h**·$(AuCl)_2$] and [**9a**·$(AuCl)_2$] are of specific interest. Complex [**1h**·$(AuCl)_2$] is the only structurally characterized complex in the current work containing a vanol-derived ligand (Figure 13), whereas compound [**9a**·$(AuCl)_2$] is the only complex containing a CycloP ligand combining a chiral R–N substituent and chiral bridge (Figure 14). The solid-state structure of this complex also shows intermolecular aurophilic interactions.

To demonstrate the generality of the coordination behavior of the chiral cyclophosphazane ligands, the reactions of **1a** with a range of other transition-metal fragments, which are of interest in catalysis, were also explored. The metal complexes [**1a**·{Rh(nbd)$Cl\}_2$] (nbd = norbornadiene) and [**1a**·{Pd(2-Me-allyl)$Cl\}_2$] were prepared by the reactions of **1a** shown in Scheme 8.

Both complexes were obtained as analytically pure solids after column chromatography and were characterized by multinuclear NMR spectroscopy, MS, and elemental analysis, and in the case of the rhodium complex, by single-crystal X-ray diffraction. The solid-state molecular structure is C_2 symmetric with each rhodium(I) atom adopting a slightly distorted square-planar geometry (Figure 15). This complex is closely related to a number of rhodium(I) compounds containing achiral cyclophosphazane ligands.[31]

^{1}H and VT ^{31}P NMR studies of complex [**1a**·{Rh(nbd)$Cl\}_2$] are consistent with the presence of rotamers with respect to the phosphorus–rhodium bonds (Scheme 9).[32] Thus, in contrast to the ^{1}H NMR spectrum of the uncoordinated ligand, which shows the expected six individual sharp resonances in the aromatic region at room temperature, the 3,3′-protons of the binol ligand in [**1a**·{Rh(nbd)$Cl\}_2$] are extremely broadened (Figure 16). The room-temperature $^{31}P\{^1H\}$ NMR spectrum shows two broad apparent doublets. As the temperature is lowered to approximately −13 °C these broad resonances are resolved into three distinct multiplets, a doublet of doublets and a doublet of doublet of doublets are ob-

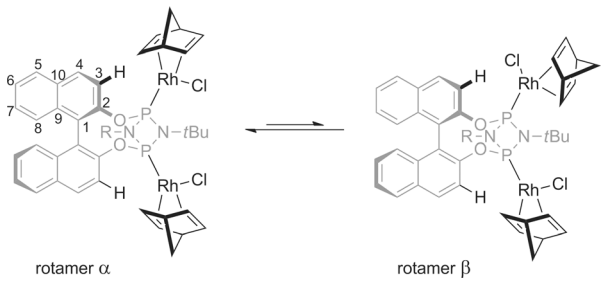

Scheme 9. Rotational isomers of **1a**·[Rh(nbd)$Cl]_2$ in solution.

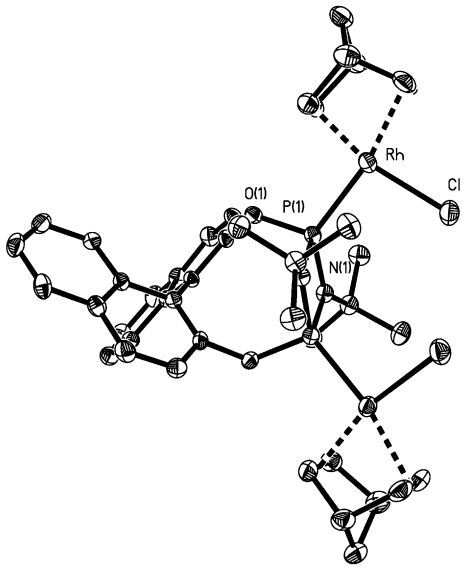

Figure 15. Molecular structure of compound [**1a**·{Rh(nbd)Cl}$_2$], thermal ellipsoids set at the 50% probability level. Hydrogen atoms are omitted for clarity. Selected bond lengths [Å] and angles [°]: P(1)–Rh 2.233(1), Rh–Cl 2.347(1), P(1)–N(1) 1.694(4); P(1′)-N(1)-P(1) 96.1(2), N(1′)-P(1)-N(1) 83.9(2).

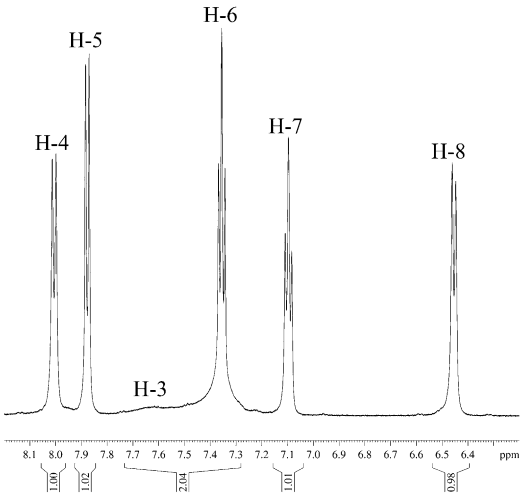

Figure 16. ^{1}H NMR spectrum of [**1a**·{Rh(nbd)Cl}$_2$] in CD_2Cl_2 at 295 K. For the atom labeling see Scheme 9.

served for the phosphorus atoms of rotamer β and a (second-order) double multiplet is found for the phosphorus atoms of rotamer α (Scheme 9 and Figure 17). The ratio of these two rotational isomers changes with the temperature, so, for example, at −13 °C the ratio of α/β is 1.2:1, whereas at −80 °C the ratio is 8:1 ($K=\alpha/\beta$, $\Delta H=(-7\pm2)$ kJ mol^{-1}, $\Delta S=(-24\pm7)$ J mol^{-1}). The bias towards the conformationally more stable α rotamer at low temperature (the observed solid-state structure of [**1a**·{Rh(nbd)Cl}$_2$], Figure 15) is as expected.

A similar dynamic situation is apparent in the palladium complex [**1a**·{Pd(2-Me-allyl)Cl}$_2$], this time, however, with a much higher rotational energy barrier. This higher energy

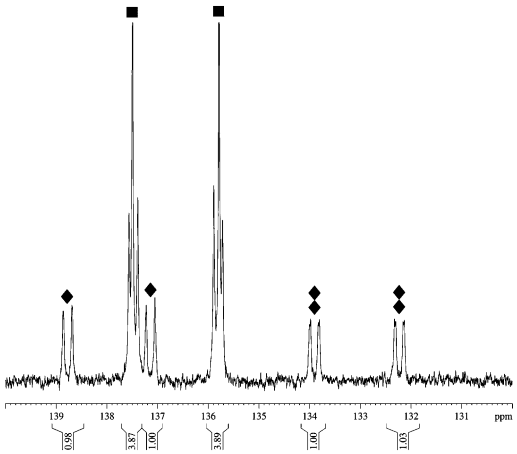

Figure 17. ^{31}P{^{1}H} NMR spectrum of [**1a**·{Rh(nbd)Cl}$_2$] in CD_2Cl_2 at 233 K. The black diamonds mark the signals corresponding to the asymmetric β isomer (P^1: $\delta=138.0$ ppm, dd, ^1J(P,Rh) = 265, ^2J(P,P) = 28 Hz; P^2: $\delta=133.1$ ppm, ddd, ^1J(P,Rh) = 272 Hz, ^2J(P,P) = 28 Hz, ^3J(P,Rh′) = 3.5 Hz); the black square denotes the C_2-symmetric rotational α isomer ($\delta=136.7$ ppm, m, ^1J(P,Rh) = 276 Hz).

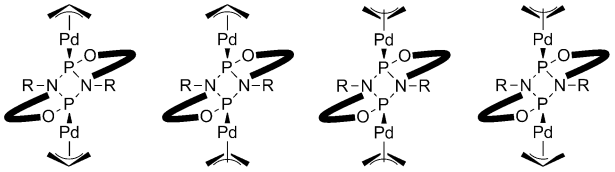

Figure 18. Illustration of the four isomeric forms of dimetallic CycloP allyl palladium complexes in solution.

barrier allows the observation of four distinct conformers in solution at room temperature (Figure 18).[33] These are also apparent in the ^{1}H NMR spectrum of [**1a**·{Pd(2-Me-allyl)Cl}$_2$] at 35 °C, showing the presence of four distinct doublet resonances for the 3,3′-protons of each isomer (Figure 19). In the room-temperature ^{13}C DEPT NMR spectrum the six resonances for the carbon atoms of the binol bridge are each split into four singlet resonances

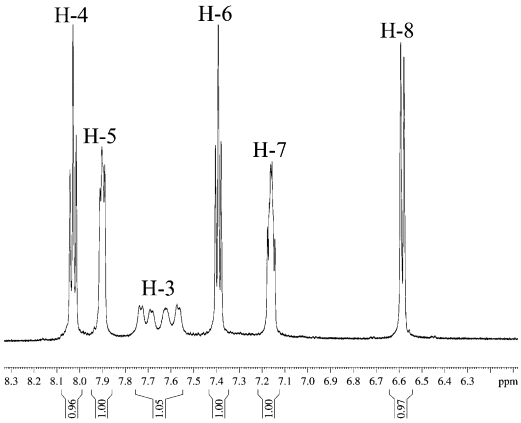

Figure 19. ^{1}H NMR spectrum of [**1a**·{Pd(2-Me-allyl)Cl}$_2$] at 310 K in CD_2Cl_2.

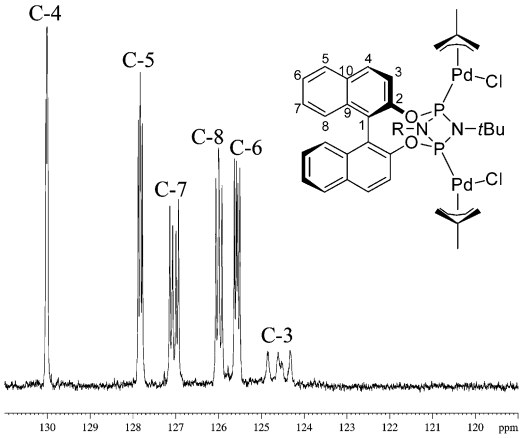

Figure 20. Aromatic section of the ^{13}C DEPT NMR spectrum of [**1a**·{Pd(2-Me-allyl)Cl}$_2$] at 295 K in CD_2Cl_2.

(Figure 20).[34] These isomers interconvert at approximately 65 °C in CD_2Cl_2 according to ^1H and ^{31}P NMR studies.[35]

Evaluation in model catalysis

Gold(I)-catalyzed cyclohydroamination of a γ-allenyl sulfonamide: Cationic gold(I) compounds are known to be exceptional catalysts for the activation of carbon–carbon multiple bonds toward nucleophilic attack and have thus been used for the formation of C–C, C–O, C–N, and C–S bonds.[36] For the purpose of assessing the activity and selectivity of the gold(I) complexes of the CycloP ligands described above, we chose the cyclohydroamination of γ-allenyl sulfonamides, which is a well understood reference reaction in the domain of gold catalysis (Scheme 10).[37] We were especially interested in the behavior of the new digold(I) species in this reaction because a wide range of di- and trinuclear gold catalysts had previously been shown to give excellent enantioselectivities in hydroamination reactions.[20,38]

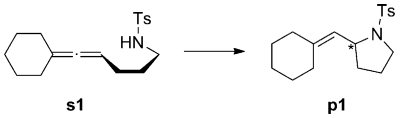

Scheme 10. Cyclohydroamination of γ-allenyl sulfonamide **s1** (Ts = tosyl).

Initially, we were interested in establishing to what extent the variation of the steric demands in the 3,3′-positions of the CycloP gold complexes might influence the reactivity and selectivity. By using literature conditions (room temperature, toluene, 5 mol% Au, 5 mol% AgOBz (Bz = benzyl)) the series of the digold(I) complexes [**1a**·(AuCl)$_2$], [**1b**·(AuCl)$_2$], [**1c**·(AuCl)$_2$], [**1e**·(AuCl)$_2$], [**1f**·(AuCl)$_2$], [**1g**·(AuCl)$_2$], and [**1h**·(AuCl)$_2$] was employed in the cyclohydroamination reference reaction (the results are shown in Table 1). The unsubstituted complex [**1a**·(AuCl)$_2$] gave full conversion after 72 h at room temperature and 19 h at 50 °C but meagre enantiomeric ratios (e.r.s) of 39:61 and 42:58 (Table 1, entries 1 and 2). We found, that gradually increasing the steric bulk of the 3,3′-positions led to a higher enantioselectivity and a concomitant retardation of the reaction rate (Table 1, entries 3–5). However, both, a further increase of the steric demand and replacement of the binol by the vanol backbone gave essentially racemic mixtures of the product in the catalytic transformation (Table 1, entries 6–8).

Table 1. Examination of the catalytic properties in the intramolecular allene hydroamination reaction.[a]

Entry	[Ligand·(AuCl)$_2$]	T [°C]	t [h]	Conv[b] [%]	e.r. R/S[c]
1	(*R*)-**1a**	25	72	98	39:61
2	(*R*)-**1a**	50	19	95	42:58
3	(*S*)-**1b**	25	93	96	39:61
4	(*R*)-**1c**	25	120	28	36:64
5	(*R*)-**1e**	25	130	83	16:84
6	(*R*)-**1f**	25	144	45	49:51
7	(*R*)-**1g**	25	144	86	49:51
8	(*R*)-**1h**	25	68	92	51:49

[a] All reactions were carried out with 5 mol% of Au^I in toluene (1 mL). [b] Conversion was monitored by ^1H NMR spectroscopy. [c] Enantioselectivities were determined by chiral HPLC.

Because the variation of the binol scaffold did not give rise to an increased selectivity, we next explored the effect of derivatization of the amine substituent, reasoning that its spatial proximity to the coordinating phosphorus atoms might have a greater impact on the selectivity. Thus, we set out to explore the influence of chirality on the amine component. By using the digold complexes of the CycloP ligands **7a**, **8a**, and **9a** in the hydroamination reaction, the selectivity was considerably increased to an e.r. of 88:12, 15:85, and 19:81, respectively (Table 2, entries 1–3).

Table 2. Examination of the catalytic properties in the intramolecular allene hydroamination reaction.[a]

Entry	[Ligand·(AuCl)$_2$]	t [h]	Conv[b] [%]	e.r. R/S[c]
1	(S_{binol},R_{amine})-**7a**	24	100	88:12
2	(R_{binol},S_{amine})-**8a**	37	99	15:85
3	(R_{binol},(1*R*,2*R*)$_{amine}$)-**9a**	16	93	19:81
4	(R_{binol},R_{amine})-**7a**	17	87	12:88
5	(*R*)-**5a**	25	87	28:72
6	(*R*)-**6a**	24	96	45:55
7	(*R*)-**11a**	45	100	23:77

[a] All reactions were carried out with 5 mol% of Au^I in toluene (1 mL) at 25 °C. [b] Conversion was monitored by ^1H NMR spectroscopy. [c] Enantioselectivities were determined by chiral HPLC.

Furthermore, to investigate possible match/mismatch effects within the CycloP scaffold the diastereomeric counterpart to [**7a**·(AuCl)$_2$] (dia-[**7a**·(AuCl)$_2$]) was prepared by inverting the chirality of the binol component. Surprisingly, this diastereomer achieved an enantiomeric ratio of 12:88 (Table 2, entry 4). In other words, both diastereomeric digold(I) complexes of ligand **7a** achieved similar enantiose-

lectivities and the absolute configuration of the enantioenriched product obtained depends solely on the chirality of the binol employed. Because the absolute configuration of the amine is not crucial to the enantioselectivity in this transformation, the achiral amine cyclophosphazane digold(I) derivatives of **5a**, **6a**, and **11a** were next employed (Table 2, entries 5–7). However, the enantioselectivities obtained in the reference reaction were considerably lowered (28:72, 45:55, and 23:77, respectively). Thus, we conclude that although the chirality of the bridging N–R group does not appear to affect the enantioselectivity there is clearly a steric influence of these groups.

Nickel(0)-catalyzed enantio- and diastereoselective coupling of a 1,4-diphenylbuta-1,3-diene and benzaldehyde: Having explored the key factors involved in the optimization of the CycloP ligand system in the gold-catalyzed cyclohydroamination reaction we decided to assess the potential of the cyclophosphazane ligands in a different late-transition-metal-catalyzed reaction. The Mori–Tamaru nickel-catalyzed coupling of 1,3-dienes and aldehydes (Scheme 11)[39] was chosen

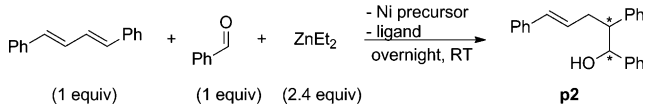

Scheme 11. Nickel(0)-catalyzed bis-homoallylation of benzaldehyde with 1,4-diphenylbutadiene and diethylzinc.

because this three-component coupling offers several distinct challenges with respect to the ligand system that were not examined in the gold(I)-catalyzed reaction; 1) unlike the gold(I)-catalyzed cyclohydroamination reaction, the coordinated nickel atom undergoes a change in the oxidation state in this transformation, 2) this transformation gives rise to two stereocenters and thus is potentially dia- and enantioselective, 3) the nickel-catalyzed reaction involves more aggressive reagents than the previously explored gold(I) reaction, and 4) this transformation is known to be catalyzed by complexes containing monodentate phosphorus ligands.[40]

The asymmetric intermolecular version of the nickel-catalyzed coupling reaction was first reported by Zhou et al. in 2007 by using substituted spirobiindane phosphoramidite ligands.[41–43] The reaction proceeds through an oxidative cyclometallation, forming an allylalkoxynickel(II) intermediate, which is subsequently re-reduced to the catalytically active nickel(0) species. Since then, several groups have broadened the scope of this reaction by using other reducing agents, which introduce alkyl, aryl, boronates, or silyl groups stereoselectively at the allylic position.[44]

Initially, the chiral ligand **7a** was employed, which gave the best enantioselectivities in the previous gold(I)-catalyzed reaction. Addition of benzaldehyde and diethylzinc to a solution of ligand **7a**, the nickel precursor [$NiBr_2$(dme)] (dme = dimethoxyethane), and 1,4-diphenylbutadiene in toluene gave the desired product after 18 h at room temperature with an enantiomeric ratio of 14:86 and an *anti*/*syn* ratio of approximately 11:1 (Table 3). A further screening of solvents showed, that other aromatic solvents such as benzene, mesitylene, and fluorobenzene gave very similar enantioselectivities, whereas more polar solvents, for example, diethylether, tetrahydrofuran, dioxane, pyridine, and acetonitrile, gave reduced enantio- and/or diastereoselectivities (see the Supporting Information). Next, the nickel precursors were varied. However, whereas nickel(II)acetylacetonate gave comparable selectivities, the enantiomeric ratio dropped to 24:76 when using the nickel(0) compound bis(cyclooctadiene)nickel.

Table 3. Examination of the catalytic properties of CycloP ligands in the Mori–Tamaru three component coupling.[a]

Entry	Ligand	*t* [h]	Conv [%][b]	*anti*/*syn*[b]	e.r. (+)/−[c]
1	(S_{binol},R_{amine})-**7a**	18	97	11:1	14:86
2[d]	(S_{binol},R_{amine})-**7a**	21	100	15:1	15:85
3[e]	(S_{binol},R_{amine})-**7a**	18	97	13:1	24:76
4	(*R*)-**5a**	20	98	10:1	91:9
5	(*R*)-**6a**	15	78	12:1	70:30
6	(R_{binol},R_{amine})-dia-**7a**	20	99	12:1	74:26
7	(R_{binol},R_{amine})-**7c**	21	100	11:1	53:47
8	(R_{binol},S_{amine})-**8a**	20	92	15:1	85:15
9	(R_{binol},(1*R*,2*R*)$_{amine}$)-**9a**	18	81	14:1	64:36
10	(R_{binol},R_{amine})-**10a**	26	55	14:1	40:60
11	(S_{binol},R_{amine})-dia-**10a**	26	95	14:1	9:91
12	(*R*)-**11a**	20	100	12:1	92:8
13	(*R*)-**1e**	21	81	11:1	88:12
14	(*R*)-**1f**	20	99	15:1	9:91
15	(*R*)-**5e**	13	26	8:1	50:50
16	(*R*)-**5h**	18	98	11:1	87:13
17	(*R*)-**7e**	13	33	8:1	50:50

[a] All reactions were carried out with 0.003 mmol CycloP ligand and 0.005 mmol of the nickel precursor at room temperature in toluene (1 mL). [b] Conversion and *anti*/*syn* ratio were determined by ^{1}H NMR spectroscopy. [c] Enantioselectivities for the major diastereomer were determined by chiral HPLC. [d] [Ni(acac)$_2$] was used. [e] [Ni(cod)$_2$] (cod = cyclooctadiene) was used.

By screening the CycloP ligands **5a**, **6a**, dia-**7a**, **7c**, **8a**, **9a**, **10a**, dia-**10a**, and **11a**, we found that the reactivity and selectivity of the nickel-catalyzed reactions depended on the cyclophosphazane scaffold used (Table 3, entries 4–12). Notably, the achiral amine-substituted binol cyclophosphazanes **5a** and **11a** gave selectivities of 9:91 and 8:92 e.r., respectively, with acceptable *anti*/*syn* ratios (Table 3, entries 4 and 12), whereas the chiral amine-derived ligands gave lower or similar selectivities (Table 3, entries 7–11). It is also noteworthy, that although both ligands **7a** and **11a** contain the same (*R*)-binol backbone but different amines, the opposite enantiomers are preferentially formed in each case. In addition, it is apparent that ligand **7a** represents the matched case, whereas the diastereomeric ligand dia-**7a** is the mismatched system (Table 3, entry 6) (cf. the gold-catalyzed reaction in which there is no distinct influence of the chirality of the amine). Due to these unexpected trends, which are markedly different or even the opposite of the gold-catalyzed reactions, the activity of the bulky binol-derived ligands **1e** and **1f** were evaluated in the nickel reference

system (Table 3, entries 13 and 14). Enantiomeric ratios of 12:88 and 9:91 were found, respectively.

Based on these results, the ligands **5e**, **5h**, and **7e** were investigated (Table 3, entries 15–17), containing bulky binol and amido groups. However, the additional steric bulk in **5e** and **7e** resulted in racemic mixtures. In contrast, the vanol derivative **5h** gave a selectivity of 87:13 e.r. These results show that the enantioselectivity is highly dependent on the steric demands of both the bridging scaffold and the amido group. This situation is similar to the gold system, which however, appears to have a lower tolerance with respect to steric congestion of the ligand.

Conclusion

The work described in this paper shows that CycloP ligands are very easily prepared by using commercially available precursors and can be elaborated extensively, by introducing chiral groups both at the bridgehead and in the amido position. These chiral phosphorus ligands are robust in solution and in the solid state and can be used to support enantioselective catalytic reactions with moderate to good enantioselectivities being observed. In the gold-catalyzed cyclohydroamination reaction the enantioselectivity is imparted by the chirality of the bridge only, whereas in the nickel-catalyzed three-component coupling reaction the enantioselectivity can be influenced by the chirality of both the bridging group and the amido groups. In both catalytic reactions extreme steric bulk of the substituent groups lowered the enantioselectivity and reaction rate. Based on the results so far it is clear that CycloP ligands are a promising family of chiral ligands. Further elaboration of these ligand sets is underway in order to improve the enantioselectivity in a number of key catalytic transformations.

Experimental Section

All manipulations, except those indicated, were carried out under exclusion of air and moisture by using standard Schlenk and glovebox techniques. As inert gas, Argon 5.0, purchased from Messer Group GmbH, was used after drying over Granusic phosphorpentoxide granulate. Solvents were dried over activated alumina columns by using a solvent purification system (M. Braun SPS 800) or according to standard literature-known methods[45] and stored in glass ampules under an argon atmosphere. Diethyl ether and *n*-pentane were distilled from sodium/potassium alloy, tetrahydrofuran, benzene, and *n*-hexane from potassium, methanol from magnesium, dichloromethane, chloroform and triethylamine from calcium hydride, and toluene from sodium. The same procedures were used to dry the deuterated solvents. Degassed solvents were obtained by three successive freeze–pump–thaw cycles. Phosphorus trichloride was distilled prior to use and triethylamine was degassed. NMR spectra were recorded on Bruker Avance (400, 500, and 600 MHz) instruments. Chemical shifts (δ) are reported in parts per million [ppm] and are referenced to residual proton solvent signals or carbon resonances.[46] H_3PO_4 (^{31}P) and CCl_3F (^{19}F) were used as external standards. The following abbreviations were used: s = singlet, d = doublet, dd = doublet of doublets, t = triplet, m = multiplet, br = broad signal. Enantioselectivities were measured on a HPLC Agilent Technologies 1200 Series instrument by using a chiral Daicel Chiracel AD-H column. High-resolution mass spectra were acquired on Bruker ApexQe hybrid 9.4 T FT-ICR (ESI) and JEOL JMS-700 magnetic sector (FAB, EI, LIFDI) spectrometers at the mass spectrometry facility of the Institute of Organic Chemistry of the University of Heidelberg. Elemental analyses were carried out in the Microanalysis Laboratory of the Heidelberg Chemistry Department. Compounds **1**·Cl_2,[47] **2**·Cl_2,[48] **3**·Cl_2,[49] **4**·Cl_2,[50] **b**,[51] **c**,[52] **1a**,[13a] and **s1**[53] were synthesized according to reported procedures. For compound numbering see the Supporting Information. All chemicals were obtained from commercial suppliers and were used without further purification.

General procedure for the synthesis of dichlorocyclophosphazanes (GP1): A solution of amine (1 equiv) and triethylamine (10 equiv) in THF was added dropwise to a solution of phosphorus trichloride (1 equiv) in THF at −78 °C. The mixture was slowly warmed to room temperature overnight (18 h). The solvent was evaporated in vacuo and the residue was extracted with toluene. The combined extracts were concentrated to a minimum amount. At this point the workup was varied depending on the compound:

Workup a) compounds 5–7, and 11: The formation of a colorless precipitate was noted during the evaporation of the solvents. In this case, the solid material was dissolved in a minimum amount of boiling toluene and then gradually cooled to room temperature. The supernatant was removed by filtration. The residue was washed with a small amount of cold toluene and *n*-pentane and dried on high vacuum to yield the dichlorocyclophosphazanes as colorless to slightly yellow solids.

Workup b) compounds 8–10: Removal of the solvent resulted in the formation of an oily residue or foam. In this case, the residue was dissolved in a small amount of toluene and layered with *n*-pentane. The mixture was then stored in the freezer (−30 or −78 °C) until the formation of a powdery precipitate was observed. The supernatant was removed by filtration and the residue was washed with *n*-pentane to yield the crude dichlorocyclophosphazane as slightly yellow or brownish solids. The dichlorocyclophosphazanes were used in the next steps without any further purification.

Data for compound 7: Colorless solid; 35% yield; ^1H NMR ([D_8]THF, 600.13 MHz, 295 K): δ = 7.89 (s, 2H; H-12), 7.86 (d, J = 8.5 Hz, 2H; H-5), 7.85–7.80 (m, 4H; H-7,H-10), 7.58–7.55 (m, 2H; H-4), 7.47–7.43 (m, 4H; H-8, H-9), 4.81–4.74 (m, 2H; H-2), 1.65 ppm (d, J = 6.7 Hz, 6H; H-1); $^{13}C\{^1H\}$ NMR ([D_8]THF, 150.92 MHz, 295 K): δ = 138.71 (m, C_{Ar}), 134.27 (s, C_{Ar}), 134.22 (s, C_{Ar}), 129.40 (s, C-5), 128.66 (s, C_{Ar}-H), 128.26 (s, C_{Ar}-H), 127.47 (s, C-12), 126.86 (s, C_{Ar}-H), 126.84 (s, C_{Ar}-H), 125.54 (s, C-4), 55.07 (t, J = 6.6 Hz, C-2), 21.74 ppm (t, J = 6.0 Hz, C-1); $^{31}P\{^1H\}$ NMR ([D_8]THF, 242.92 MHz, 295 K): δ = 219.35 ppm (s); MS (LIFDI(+)): m/z (100%) calcd for $C_{24}H_{22}Cl_2N_2P_2$: 470.1; found 469.8 $[M]^+$; elemental analysis calcd (%) for $C_{24}H_{22}N_2P_2Cl_2$: C 61.16, H 4.71, N 5.94; found: C 61.08, H 4.84, N 5.95. The spectroscopic data for the dichlorocyclophosphazanes **5**, **6**, **8**, **9**, **10**, and **11** can be found in the Supporting Information.

General procedure for the synthesis of CycloP ligands (GP2): A solution of the diol (1 equiv) and triethylamine (10 equiv) in toluene was added to a solution of the dichlorocyclophosphazane (1 equiv) in toluene at room temperature. The resulting mixture was heated to 110 °C overnight (18 h), cooled to room temperature, and filtered. The obtained solid was then purified by column chromatography (SiO_2, *n*-pentane/ethyl acetate) to obtain the pure CycloP ligands as colorless or pale yellow solids.

Data for 1b: Colorless solid; 40% yield; ^1H NMR (C_6D_6, 600.13 MHz, 295 K): δ = 8.04 (s, 2H; H-4), 7.33 (d, J = 8.16 Hz, 2H; H-6), 6.95–6.91 (m, 2H; H-7), 6.79 (d, J = 8.65 Hz, 2H; H-9), 6.71–6.67 (m, 2H; H-8), 0.94 ppm (s, 18H; H-12); $^{13}C\{^1H\}$ NMR (C_6D_6, 150.92 MHz, 295 K): δ = 149.23 (m, C_{Ar}), 134.19 (s, C_{Ar}), 132.61 (s, C-4), 131.36 (s, C_{Ar}), 128.35 (s, C_{Ar}), 127.47 (s, C-8), 127.02 (s, C-6), 126.09 (s, C-9), 125.78 (s, C-7), 119.49 (s, C-3), 52.89 (t, J = 12.15 Hz, C-11), 31.01 ppm (t, J = 6.60 Hz, C-12); $^{31}P\{^1H\}$ NMR (C_6D_6, 242.92 MHz, 295 K): δ = 177.31 ppm (s); HRMS (ESI(+)):m/z (9%) calcd for $C_{28}H_{29}Br_2N_2O_2P_2$: 645.0071; found 645.0058 $[M+H]^+$; elemental analysis calcd (%) for $C_{28}H_{28}N_2O_2P_2Br_2$: C 52.04, H 4.37, N 4.33; found: C 52.07, H 4.41, N 4.36. The spectroscopic data for the CycloP ligands **1c**, **1e**, **1f**, **1g**, **1h**, **2a**, **3a**, **5a**, **5e**, **5h**, **6a**, **7a**, **7c**, **7e**, **8a**, **9a**, **10a**, and **11a** can be found in the Supporting Information.

General procedure for the synthesis of digold(I) CycloP metal complexes (GP3): Dimethylsulfidegold(I) chloride (2 equiv) was added in one portion to a solution of the CycloP ligand (1 equiv) in dichloromethane. The clear solution was stirred at room temperature for 30 min, then the solvent was removed and the residue was recrystallized from dichloromethane/*n*-pentane. The colorless solid was washed with *n*-pentane and dried on high vacuum to yield the digold(I) CycloP complex as a colorless solid.

Data for [1a·(AuCl)$_2$]: Colorless solid; 76% yield; ^{1}H NMR ($CDCl_3$, 500.05 MHz, 300 K): $\delta = 8.06$ (d, $J = 8.91$ Hz, 2H; H-4), 7.91 (d, $J = 8.11$ Hz, 2H; H-6), 7.48 (d, $J = 8.94$ Hz, 2H; H-3), 7.47–7.42 (m, 2H; H-7), 7.22–7.18 (m, 2H; H-8), 6.47 (d, $J = 8.57$ Hz, 2H; H-9), 1.24 ppm (s, 18H; H-12); ^{13}C{^{1}H} NMR ($CDCl_3$, 125.74 MHz, 300 K): $\delta = 148.83$ (m, C_{Ar}), 134.57 (s, C_{Ar}), 131.53 (s, C_{Ar}), 131.12 (s, C-4), 128.24 (s, C-8), 128.17 (s, C-6), 126.79 (s, C-7), 125.92 (s, C-9), 124.66 (m, C_{Ar}), 123.25 (s, C-3), 56.45 (t, $J = 2.21$ Hz, C-11), 31.44 ppm (t, $J = 5.19$ Hz, C-12); ^{31}P{^{1}H} NMR ($CDCl_3$, 242.92 MHz, 295 K): $\delta = 119.14$ ppm (s); HRMS (ESI(+)): *m/z* (4%) calcd for $C_{28}H_{30}Au_2Cl_2N_2O_2P_2Na$: 975.0388; found 975.0357 $[M+a]^+$; elemental analysis calcd (%) for $C_{28}H_{30}N_2O_2P_2Au_2Cl_2$: C 35.28, H 3.17, N 2.94; found: C 34.91, H 3.30, N 2.81.

The spectroscopic data for the CycloP complexes [**1b**·(AuCl)$_2$], [**1c**·(AuCl)$_2$], [**1e**·(AuCl)$_2$], [**1f**·(AuCl)$_2$], [**1g**·(AuCl)$_2$], [**1h**·(AuCl)$_2$], [**5a**·(AuCl)$_2$], [**6a**·(AuCl)$_2$], [**7a**·(AuCl)$_2$], dia-[**7a**·(AuCl)$_2$], [**8a**·(AuCl)$_2$], [**9a**·(AuCl)$_2$], and [**11a**·(AuCl)$_2$] can be found in the Supporting Information.

Synthesis of the dirhodium(I) CycloP complex [1a·{Rh(nbd)Cl}$_2$]: Dry dichloromethane (15 mL) was added to a Schlenk flask containing the CycloP ligand **1a** (347 mg, 0.753 mmol, 1 equiv) and [Rh(nbd)Cl]$_2$ (368 mg, 0.753 mmol, 1 equiv) and the mixture was stirred at room temperature overnight. The solvent was removed and the residue was purified by column chromatography (SiO_2, *n*-pentane/ethyl acetate = 1:1 to pure ethyl acetate) to give the dirhodium(I) CycloP complex as an orange solid (487 mg, 68%). Single crystals suitable for X-ray diffraction analysis were grown by carefully layering a solution of the complex in dichloromethane with *n*-pentane. ^{1}H NMR (CD_2Cl_2, 600.13 MHz, 295 K): $\delta = 8.01$ (d, $J = 8.81$ Hz, 2H; H-4), 7.88 (d, $J = 8.15$ Hz, 2H; H-6), 7.76–7.25 (m, 4H; H-3, H-7), 7.13–7.07 (m, 2H; H-8), 6.45 (d, $J = 8.42$ Hz, 2H; H-9), 5.62–4.92 (m, 4H; H-14, H-15), 4.29–3.62 (m, 8H; H-13, H-16, H-17, H-18), 1.65–1.46 (m, 4H; H-19), 1.41–1.23 ppm (m, 18H; H-12); ^{13}C{^{1}H} NMR (CD_2Cl_2, 150.92 MHz, 295 K): $\delta = 151.43$–150.22 (m, C_{Ar}), 134.95 (s, C_{Ar}), 131.25 (s, C_{Ar}), 129.96 (s, C-4), 128.12 (s, C-6), 127.20 (m, C-8), 126.18 (s, C-9), 125.67 (m, C-7, C_{Ar}), 124.26 (m, C-3), 94.35–87.31 (m, C-14, C-15), 65.18 (m, C-19), 57.22–55.39 (m, C_{nbd}), 54.66 (m, C-11); 51.54–47.61 (m, C_{nbd}), 33.30–30.64 ppm (m, C-12); due to significant broadening and overlapping of the ^{13}C resonances the signals were assigned by analogy to the previously reported [RhCl(nbd)(phosphoramidite)] complexes by Albinati and coworkers;[32] ^{31}P{^{1}H} NMR (CD_2Cl_2, 242.92 MHz, 295 K): $\delta = 138.82$–136.17 (m, ≈ 1.5 P), 134.78–132.23 ppm (m, ≈ 0.5 P); for comparison: a low-temperature ^{31}P{^{1}H} NMR spectrum ($T = 233$ K) comprising of sharp resolved resonances is shown in Figure 17; HRMS (FAB(+)):*m/z* (100%) calcd for $C_{42}H_{46}ClN_2O_2P_2Rh_2$: 913.0833; found: 913.0892 $[M-Cl]^+$; elemental analysis calcd (%) for $C_{42}H_{46}N_2O_2P_2Rh_2Cl_2$: C 53.13, H 4.88, N 2.95; found C 52.63, H 4.94, N 3.05.

The spectroscopic data for the CycloP complex [**1a**·{Pd(2-Me-allyl)Cl}$_2$] can be found in the Supporting Information.

Gold-catalyzed cyclohydroamination: A mixture of the digold(I) complex (0.0025 mmol) and the corresponding silver(I) salt (0.005 mmol) in toluene (dry and degassed, 0.5 mL) was stirred at room temperature for 15 min in the dark. Then, a solution of the γ-allenyl sulfonamide **s1** (0.1 mmol) in toluene (dry and degassed, 0.5 mL) was added and the reaction mixture was left to stir at room temperature for the indicated time. The progress of the reaction was monitored by ^{1}H NMR spectroscopy. Upon completion, the crude mixture was loaded directly onto a silica gel column and purified by column chromatography (SiO_2, *n*-pentane/ethyl acetate = 5:1) to yield the cyclized product **p1**. Spectroscopic properties of **p1** were in accordance to previous reports in the literature.[37b] Enantioselectivities for **p1** were determined by chiral HPLC employing a Daicel Chiracel AD-H column: conditions: *n*-hexane/isopropanol = 95:5, 20 °C, 1 mL min^{-1}, $t_{(S)} = 13.6$, $t_{(R)} = 14.9$ min.

Nickel-catalyzed three-component coupling: This reaction was conducted similarly as described previously by Zhou et al.[41] Benzaldehyde (0.2 mmol) was added to a solution of the CycloP ligand (0.003 mmol), [$NiBr_2$(dme)] (0.005 mmol) and *trans*,*trans*-1,4-diphenyl-1,3-butadiene (0.1 mmol) in the indicated solvent (1 mL). The solution was stirred at room temperature for 5 min and then a 1 M solution of diethylzinc in hexane (0.24 mmol) was added dropwise. The reaction mixture was stirred for the indicated time at room temperature and then quenched by the addition of 1 M HCl. Extraction with ethyl acetate, washing with saturated aqueous $NaHCO_3$ solution and evaporation of the solvent yielded the crude coupling product **p2**. From this crude mixture the diastereomeric ratio was determined by ^{1}H NMR spectroscopy, then the solid was further purified by column chromatography (SiO_2, *n*-pentane/ethyl acetate = 4:1). Spectroscopic properties of **p2** were in accordance to previous reports in the literature.[41] Enantioselectivities for product **p2** were determined by chiral HPLC employing a Daicel Chiracel AD-H column: conditions: *n*-hexane/isopropanol = 95:5, 20 °C, 1 mL min^{-1}, $t_{(+)} = 17.1$, $t_{(-)} = 19.7$ min.

X-ray crystal structure determinations: Crystal data and details of the structure determinations are listed in the Supporting Information. Intensity data were collected at low temperature with a Bruker AXS Smart 1000 ($Mo_{K\alpha}$ radiation, sealed tube, graphite monochromator), an Agilent Technologies Supernova-E ($Mo_{K\alpha}$ or $Cu_{K\alpha}$ radiation, microfocus tube, multilayer mirror optics), a Nonius Kappa CCD diffractometer ($Mo_{K\alpha}$ radiation, sealed tube, graphite monochromator) or a Bruker AXS Smart X2S ($Mo_{K\alpha}$ radiation, sealed microfocus tube, silicon monochromator) CCD diffractometers. Data were corrected for air and detector absorption, Lorentz and polarization effects;[54–56] absorption by the crystal was treated analytically,[55,57] numerically (Gaussian grid)[55] or with a semiempirical multiscan method.[56,58–60] The structures were solved by the charge flip procedure,[61] by the heavy-atom method combined with structure expansion by direct methods applied to difference structure factors,[62] by direct methods with dual-space recycling,[63,64] or by conventional direct methods.[65–67] Refinement was carried out by full-matrix least-squares methods based on F^2 against all unique reflections.[66,68] All non-hydrogen atoms were given anisotropic displacement parameters. Hydrogen atoms were generally input at calculated positions and refined with a riding model. When justified by the quality of the data the positions of some hydrogen atoms were taken from difference Fourier syntheses and refined. When found necessary, disordered groups and/or solvent molecules where subjected to suitable geometry and adp restraints. Due to severe disorder and fractional occupancy, electron density attributed to solvent of crystallization was removed from the structures of **1h**·[AuCl]$_2$ and **9a**·[AuCl]$_2$ with the BYPASS procedure,[69] as implemented in PLATON (SQUEEZE).[70] Partial structure factors from the solvent masks were included in the refinement as separate contributions to F_{obs}.

CCDC-939645 (**A**), 939646 ([**A**·(AuCl)$_2$]), 939647 ([**1a**·(AuCl)$_2$]), 939648 ([**1a**·{Rh(nbd)Cl}$_2$]), 939649 (**1b**), 939650 ([**1b**·(AuCl)$_2$]), 939651 (**1c**), 939652 ([**1c**·(AuCl)$_2$]), 939653 ([**1e**·(AuCl)$_2$]), 939654 ([**1g**·(AuCl)$_2$]), 939655 ([**1h**·(AuCl)$_2$]), 939656 (**2a**), 939657 (**5a**), 939658 (**6**·Cl$_2$), 939659 (**6a**), 939660 (**7c**), 939661 ([**9a**·(AuCl)$_2$]), 939662 ((R_{binol},R_{amine})-**10a**), and 939663 ((S_{binol},R_{amine})-**10a**) contain the supplementary crystallographic data for this paper. These data can be obtained free of charge from The Cambridge Crystallographic Data Centre via www.ccdc.cam.ac.uk/data_request/cif.

Acknowledgements

We gratefully acknowledge the EU (Erasmus-Program (T.R.), ERC-Advanced Investigator Grant (D.S.W.)] and the award of a Ph.D. grant to T.R. from the Landesgraduiertenförderung (LGF Funding Program of the state of Baden-Württemberg). This work has also been funded by the DFG (SFB 623, TP B6). We also thank Y. Lv and Dr. J. E. Davies (Cam-

bridge) for collecting X-ray data on selected compounds and Dr. J. Graf (Heidelberg) for recording $^{13}C\{^{31}P\}$ NMR spectra.

[1] a) A. Börner in *Phosphorus Ligands in Asymmetric Catalysis, Vols. 1–3*, 1st ed., Wiley-VCH, Weinheim, **2008**; b) H.-U. Blaser, H.-J. Federsel in *Asymmetric Catalysis on Industrial Scale: Challenges, Approaches and Solutions*, 2nd ed., Wiley-VCH, Weinheim, **2010**; c) A. Behr, P. Neubert in *Applied Homogeneous Catalysis*, 1st ed., Wiley-VCH, Weinheim, **2012**; d) P. W. N. M. van Leeuwen, J. C. Chadwick in *Homogeneous Catalysts*, 1st ed., Wiley-VCH, Weinheim, **2011**; e) P. C. J. Kamer, P. W. N. M. van Leeuwen in *Phosphorus(III) Ligands in Homogeneous Catalysis*, 1st ed., Wiley, New York, **2012**; f) V. Caprio, J. Williams in *Catalysis in Asymmetric Synthesis*, 2nd ed., Wiley, New York, **2009**; g) I. Ojima in *Catalytic Asymmetric Synthesis* 3rd ed., Wiley, New York, **2010**; h) M. Gruttadauria, F. Giacalone in *Catalytic Methods in Asymmetric Synthesis: Advanced Materials, Techniques and Applications*, 1st ed., Wiley, New York, **2011**.

[2] a) W. S. Knowles, *Angew. Chem.* **2002**, *114*, 2096–2107; *Angew. Chem. Int. Ed.* **2002**, *41*, 1998–2007; b) W. S. Knowles, M. J. Sabacky, *Chem. Commun. (London)* **1968**, 1445–1446; c) W. S. Knowles, M. J. Sabacky, B. D. Vineyard, *J. Chem. Soc. Chem. Commun.* **1972**, *10*–11.

[3] L. Horner, H. Siegel, H. Büthe, *Angew. Chem.* **1968**, *80*, 1034; *Angew. Chem. Int. Ed. Engl.* **1968**, *7*, 942.

[4] a) T.-P. Dang, H. B. Kagan, *J. Chem. Soc. D* **1971**, 481; b) H. B. Kagan, T.-P. Dang, *J. Am. Chem. Soc.* **1972**, *94*, 6429–6433; c) F. Lagasse, H. B. Kagan, *Chem. Pharm. Bull.* **2000**, *48*, 315–324.

[5] A. Alexakis, J. Frutos, P. Mangeney, *Tetrahedron: Asymmetry* **1993**, *4*, 2427–2430.

[6] a) A. H. M. de Vries, A. Meetsma, B. L. Feringa, *Angew. Chem.* **1996**, *108*, 2526–2528; *Angew. Chem. Int. Ed. Engl.* **1996**, *35*, 2374–2376; b) B. L. Feringa, M. Pineschi, L. A. Arnold, R. Imbos, A. H. M. de Vries, *Angew. Chem.* **1997**, *109*, 2733–2736; *Angew. Chem. Int. Ed. Engl.* **1997**, *36*, 2620–2623; c) M. van den Berg, A. J. Minnaard, E. P. Schudde, J. van Esch, A. H. M. de Vries, J. G. de Vries, B. L. Feringa, *J. Am. Chem. Soc.* **2000**, *122*, 11539–11540.

[7] a) M. T. Reetz, T. Sell, *Tetrahedron Lett.* **2000**, *41*, 6333; b) M. T. Reetz, G. Mehler, *Angew. Chem.* **2000**, *112*, 4047–4049; *Angew. Chem. Int. Ed.* **2000**, *39*, 3889–3890.

[8] C. Claver, E. Fernandez, A. Gillon, K. Heslop, D. J. Hyett, A. Martorell, A. G. Orpen, P. G. Pringle, *Chem. Commun.* **2000**, 961.

[9] a) J. F. Teichert, B. L. Feringa, *Angew. Chem.* **2010**, *122*, 2538–2582; *Angew. Chem. Int. Ed.* **2010**, *49*, 2486–2528; b) I. V. Komarov, A. Börner, *Angew. Chem.* **2001**, *113*, 1237–1240; *Angew. Chem. Int. Ed.* **2001**, *40*, 1197–1200.

[10] a) Q.-L. Zhou in *Privileged Chiral Ligands and Catalysts*, 1st ed., Wiley-VCH, Weinheim, **2011**; b) T. P. Yoon, E. N. Jacobsen, *Science* **2003**, *299*, 1691–1693.

[11] R. Keat, D. G. Thompson, *Angew. Chem.* **1977**, *89*, 829–829; *Angew. Chem. Int. Ed. Engl.* **1977**, *16*, 797–798.

[12] a) M. Vijjulatha, S. Kumaraswamy, K. C. K. Swamy, U. Engelhardt, *Polyhedron* **1999**, *18*, 2557–2562; b) K. P. Kumar, M. Chakravarty, K. C. K. Swamy, *Z. Anorg. Allg. Chem.* **2004**, *630*, 2063–2070.

[13] a) M. Chakravarty, P. Kommana, K. C. K. Swamy, *Chem. Commun.* **2005**, 5396–5398; b) K. C. Kumara Swamy, G. Gangadhararao, V. Srinivas, N. N. B. Kumar, E. Balaraman, M. Chakravarty, *Inorg. Chim. Acta* **2011**, *372*, 374–382.

[14] a) K. C. Kumara Swamy, G. Gangadhararao, R. R. Suresh, N. N. B. Kumar, M. Chakravarty, *J. Organomet. Chem.* **2010**, *695*, 1042–1051; b) R. Rama Suresh, K. C. K. Swamy, *Tetrahedron Lett.* **2009**, *50*, 6004–6007; c) S. Mohanty, M. S. Balakrishna, *J. Chem. Sci.* **2010**, *122*, 137–142.

[15] a) L. Stahl, *Coord. Chem. Rev.* **2000**, *210*, 203–250; b) G. G. Briand, T. Chivers, M. Krahn, *Coord. Chem. Rev.* **2002**, *233–234*, 237–254.

[16] a) K. V. Axenov, V. V. Kotov, M. Klinga, M. Leskelä, T. Repo, *Eur. J. Inorg. Chem.* **2004**, 695–706; b) K. V. Axenov, M. Klinga, M. Leskelä, V. Kotov, T. Repo, *Eur. J. Inorg. Chem.* **2004**, 4702–4709; c) K. V. Axenov, M. Leskelä, T. Repo, *J. Catal.* **2006**, *238*, 196–205; d) K. V. Axenov, I. Kilpeläinen, M. Klinga, M. Leskelä, T. Repo, *Organometallics* **2006**, *25*, 463–471; e) K. V. Axenov, M. Klinga, O. Lehtonen, H. T. Koskela, M. Leskelä, T. Repo, *Organometallics* **2007**, *26*, 1444–1460; f) D. F. Moser, L. Grocholl, L. Stahl, R. J. Staples, *Dalton Trans.* **2003**, 1402–1410.

[17] A chelating behavior of dichlorocyclophosphazanes has been proposed previously, however, the evidence appears weak by modern standards: a) N. Kuhn, M. Winter, *J. Organomet. Chem.* **1983**, *243*, C47–C50; b) L. S. Jenkins, G. R. Willey, *J. Chem. Soc. Dalton Trans.* **1979**, 777–780.

[18] a) J. Park, S. Hong, *Chem. Soc. Rev.* **2012**, *41*, 6931–6943; b) M. Shibasaki, M. Kanai, S. Matsunaga, N. Kumagai, *Acc. Chem. Res.* **2009**, *42*, 1117–1127; c) E. K. Van den Beuken, B. L. Feringa, *Tetrahedron* **1998**, *54*, 12985–13011; d) S. Matsunaga, M. Shibasaki, *Bull. Chem. Soc. Jpn.* **2008**, *81*, 60–75; e) M. Shibasaki, Y. Yamamoto in *Multimetallic Catalysts in Organic Synthesis*, 1st ed., Wiley-VCH, Weinheim, **2004**; f) J.-A. Ma, D. Cahard, *Angew. Chem.* **2004**, *116*, 4666–4683; *Angew. Chem. Int. Ed.* **2004**, *43*, 4566–4583; g) A. E. Allen, D. W. C. MacMillan, *Chem. Sci.* **2012**, *3*, 633–658.

[19] a) H. Steinhagen, G. Helmchen, *Angew. Chem.* **1996**, *108*, 2489–2492; *Angew. Chem. Int. Ed. Engl.* **1996**, *35*, 2339–2342; b) J. Weston, *Chem. Rev.* **2005**, *105*, 2151–2174.

[20] L.-I. Rodríguez, T. Roth, J. Lloret Fillol, H. Wadepohl, L. H. Gade, *Chem. Eur. J.* **2012**, *18*, 3721–3728.

[21] For a selection see: a) O. J. Scherer, P. Klusmann, *Angew. Chem.* **1969**, *81*, 743–744; *Angew. Chem. Int. Ed. Engl.* **1969**, *8*, 752–753; b) A. Bashall, E. L. Doyle, F. García, G. T. Lawson, D. J. Linton, D. Moncrieff, M. McPartlin, A. D. Woods, D. S. Wright, *Chem. Eur. J.* **2002**, *8*, 5723–5731; c) R. Kuzora, A. Schulz, A. Villinger, R. Wustrack, *Dalton Trans.* **2009**, 9304–9311; d) F. Reiß, A. Schulz, A. Villinger, N. Weding, *Dalton Trans.* **2010**, *39*, 9962–9972; e) J.-T. Ahlemann, H. W. Roesky, R. Murugavel, E. Parisini, M. Noltemeyer, H.-G. Schmidt, O. Müller, R. Herbst-Irmer, L. N. Markovskii, Y. G. Shermolovich, *Chem. Ber.* **1997**, *130*, 1113–1121.

[22] a) T. Chivers, I. Manners in *Inorganic Rings and Polymers of the P-Block Elements*, RSC Publishing, Cambridge, **2009**, pp. 231–252; b) E. W. Abel, D. A. Armitage, G. R. Willey, *J. Chem. Soc.* **1965**, 57–61; c) D. A. Harvey, R. Keat, D. S. Rycroft, *J. Chem. Soc. Dalton Trans.* **1983**, 425–431; d) R. Murugavel, S. S. Krishnamurthy, J. Chandrasekhar, M. Nethaji, *Inorg. Chem.* **1993**, *32*, 5447–5453; e) F. García, R. A. Kowenicki, L. Riera, D. S. Wright, *Dalton Trans.* **2005**, 2495–2496; f) W. Zeiss, W. Schwarz, H. Hess, *Angew. Chem.* **1977**, *89*, 423–424; *Angew. Chem. Int. Ed. Engl.* **1977**, *16*, 407–408; g) S. Karthikeyan, K. Vyas, S. S. Krishnamurthy, T. S. Cameron, B. R. Vincent, *J. Chem. Soc. Dalton Trans.* **1988**, 1371–1375; h) C. Malavaud, T. N. M′Pondo, L. Lopez, J. Barrans, J.-P. Legros, *Can. J. Chem.* **1984**, *62*, 43–50; i) G. B. Ansell, G. J. Bullen, *J. Chem. Soc. A* **1968**, 3026–3036.

[23] a) I. Silaghi-Dumitrescu, I. Haiduc, *Phosphorus Sulfur Silicon Relat. Elem.* **1994**, *91*, 21–36; b) R. Keat, *Top. Curr. Chem.* **1982**, *102*, 89–116; c) M. S. Balakrishna, D. J. Eisler, T. Chivers, *Chem. Soc. Rev.* **2007**, *36*, 650–664.

[24] Examples in P^{III}–N chemistry: a) A. D. Bond, E. L. Doyle, F. García, R. A. Kowenicki, M. McPartlin, L. Riera, D. S. Wright, *Chem. Commun.* **2003**, 2990–2991; b) see reference [21]; example in P^{V}–N chemistry: c) E. Fluck, D. Wachtler, *Liebigs Ann. Chem.* **1980**, 1651–1658.

[25] a) F. Dodds, F. García, R. A. Kowenicki, M. McPartlin, L. Riera, A. Steiner, D. S. Wright, *Chem. Commun.* **2005**, 5041–5043; b) F. García, R. A. Kowenicki, I. Kuzu, L. Riera, M. McPartlin, D. S. Wright, *Dalton Trans.* **2004**, 2904–2909.

[26] a) L. Wang, W. Meng, C.-L. Zhu, Y. Zheng, J. Nie, J.-A. Ma, *Angew. Chem.* **2011**, *123*, 9614–9618; *Angew. Chem. Int. Ed.* **2011**, *50*, 9442–9446; b) A. Z. González, D. Benitez, E. Tkatchouk, W. A. Goddard III, F. D. Toste, *J. Am. Chem. Soc.* **2011**, *133*, 5500–5507; c) I. Alonso, B. Trillo, F. López, S. Montserrat, G. Ujaque, L. Castedo, A. Lledós, J. L. Mascareñas, *J. Am. Chem. Soc.* **2009**, *131*, 13020–13030; d) A. Z. González, F. D. Toste, *Org. Lett.* **2010**, *12*, 200–203;

e) M. T. Reetz, J.-A. Ma, R. Goddard, *Angew. Chem.* **2005**, *117*, 416–419; *Angew. Chem. Int. Ed.* **2005**, *44*, 412–415.

[27] a) N. Burford, T. S. Cameron, K. D. Conroy, B. Ellis, M. Lumsden, C. L. B. Macdonald, R. McDonald, A. D. Phillips, P. J. Ragogna, R. W. Schurko, D. Walsh, R. E. Wasylishen, *J. Am. Chem. Soc.* **2002**, *124*, 14012–14013; b) N. Burford, K. D. Conroy, J. C. Landry, P. J. Ragogna, M. J. Ferguson, R. McDonald, *Inorg. Chem.* **2004**, *43*, 8245–8251; c) N. Burford, J. C. Landry, M. J. Ferguson, R. McDonald, *Inorg. Chem.* **2005**, *44*, 5897–5902.

[28] a) M. S. Balakrishna, V. S. Reddy, S. S. Krishnamurthy, *Coord. Chem. Rev.* **1994**, *129*, 1–90; b) S. S. Krishnamurthy, V. S. Reddy, A. Chandrasekaran, M. Nethaji, *Phosphorus Sulfur Silicon Relat. Elem.* **1992**, *64*, 99–106; c) M. S. Balakrishna, *J. Organomet. Chem.* **2010**, *695*, 925–936.

[29] a) H. Schmidbaur, *Gold Bull.* **2000**, *33*, 3–10; b) H. Schmidbaur, A. Schier, *Chem. Soc. Rev.* **2008**, *37*, 1931–1951; c) H. Schmidbaur, A. Schier, *Chem. Soc. Rev.* **2012**, *41*, 370–412.

[30] a) R. Martin, S. L. Buchwald, *Acc. Chem. Res.* **2008**, *41*, 1461–1473; b) W. Wang, G. B. Hammond, B. Xu, *J. Am. Chem. Soc.* **2012**, *134*, 5697–5705.

[31] a) M. S. Balakrishna, S. S. Krishnamurthy, *J. Organomet. Chem.* **1992**, *424*, 243–251; b) M. S. Balakrishna, D. Suresh, J. T. Mague, *J. Chem. Sci.* **2011**, *123*, 861–868.

[32] S. Filipuzzi, E. Männel, P. S. Pregosin, A. Albinati, S. Rizzato, L. F. Veiros, *Organometallics* **2008**, *27*, 4580–4588.

[33] S. Filipuzzi, P. S. Pregosin, A. Albinati, S. Rizzato, *Organometallics* **2006**, *25*, 5955–5964.

[34] This is not due to ^{31}P–^{13}C coupling because a $^{13}C\{^{31}P\}$ NMR spectrum also shows the same splitting pattern.

[35] Several other metal precursor compounds were investigated on the NMR scale, for example, $[\{Ir(cod)Cl\}_2]$ and $[(Me_2S)CuBr]$. In contrast to the behavior of the rhodium complex, the corresponding iridium complex did not show fluxional properties at room temperature. The copper complex shows similar NMR behavior to [**1a**·$(AuCl)_2$] but was only soluble in DMSO.

[36] a) A. S. K. Hashmi, F. D. Toste in *Modern Gold-Catalyzed Synthesis* 1st ed., Wiley-VCH, Weinheim, **2012**; b) N. Krause, C. Winter, *Chem. Rev.* **2011**, *111*, 1994–2009; c) A. Fürstner, P. W. Davies, *Angew. Chem.* **2007**, *119*, 3478–3519; *Angew. Chem. Int. Ed.* **2007**, *46*, 3410–3449; d) C. F. Bender, R. A. Widenhoefer, *Chem. Commun.* **2008**, 2741–2743; e) X. Q. Han, R. A. Widenhoefer, *Angew. Chem.* **2006**, *118*, 1779–1781; *Angew. Chem. Int. Ed.* **2006**, *45*, 1747–1749; f) R. A. Widenhoefer, X. Han, *Eur. J. Org. Chem.* **2006**, 4555–4563.

[37] a) N. Krause, A. S. K. Hashmi in *Modern Allene Chemistry, Vols. 1 and 2*, Wiley-VCH, Weinheim, **2004**; b) R. L. LaLonde, B. D. Sherry, E. J. Kang, F. D. Toste, *J. Am. Chem. Soc.* **2007**, *129*, 2452–2453; c) Z. Zhang, C. F. Bender, R. A. Widenhoefer, *Org. Lett.* **2007**, *9*, 2887–2889; d) H. Teller, M. Corbet, L. Mantilli, G. Gopakumar, R. Goddard, W. Thiel, A. Fürstner, *J. Am. Chem. Soc.* **2012**, *134*, 15331–15342.

[38] a) M.-Z. Wang, C.-Y. Zhou, Z. Guo, E. L.-M. Wong, M.-K. Wong, C.-M. Che, *Chem. Asian J.* **2011**, *6*, 812–824; b) E. Tkatchouk, N. P. Mankad, D. Benitez, W. A. Goddard III, F. D. Toste, *J. Am. Chem. Soc.* **2011**, *133*, 14293–14300; c) F. Liu, D. Qian, L. Li, X. Zhao, J. Zhang, *Angew. Chem.* **2010**, *122*, 6819–6822; *Angew. Chem. Int. Ed.* **2010**, *49*, 6669–6672.

[39] a) Y. Tamaru in *Modern Organonickel Chemistry*, 1st ed., Wiley-VCH, Weinheim, **2005**; b) H. Clavier, H. Pellissier, *Adv. Synth. Catal.* **2012**, *354*, 3347–3403; c) J. Montgomery, *Angew. Chem.* **2004**, *116*, 3980–3998; *Angew. Chem. Int. Ed.* **2004**, *43*, 3890–3908; d) Y. Sato, M. Takimoto, K. Hayashi, T. Katsuhara, K. Takagi, M. Mori, *J. Am. Chem. Soc.* **1994**, *116*, 9771–9772; e) M. Kimura, A. Ezoe, K. Shibata, Y. Tamaru, *J. Am. Chem. Soc.* **1998**, *120*, 4033–4034; f) M. Kimura, H. Fujimatsu, A. Ezoe, K. Shibata, M. Shimizu, S. Matsumoto, Y. Tamaru, *Angew. Chem.* **1999**, *111*, 410–413; *Angew. Chem. Int. Ed.* **1999**, *38*, 397–400; g) Y. Sato, M. Takimoto, M. Mori, *Tetrahedron Lett.* **1996**, *37*, 887–890; h) M. Kimura, A. Ezoe, M. Mori, K. Iwata, Y. Tamaru, *J. Am. Chem. Soc.* **2006**, *128*, 8559–8568.

[40] S. Ogoshi, K.-I. Tonomori, M.-A. Oka, H. Kurosawa, *J. Am. Chem. Soc.* **2006**, *128*, 7077–7086.

[41] Y. Yang, S.-F. Zhu, H.-F. Duan, C.-Y. Zhou, L.-X. Wang, Q.-L. Zhou, *J. Am. Chem. Soc.* **2007**, *129*, 2248–2249.

[42] Y. Sato, Y. Hinata, R. Seki, Y. Oonishi, N. Saito, *Org. Lett.* **2007**, *9*, 5597–5599.

[43] An asymmetric intramolecular reaction was described recently: a) Y. Sato, N. Saito, M. Mori, *J. Am. Chem. Soc.* **2000**, *122*, 2371–2372; b) Y. Sato, N. Saito, M. Mori, *J. Org. Chem.* **2002**, *67*, 9310–9317; c) M. Takimoto, Y. Kajima, Y. Sato, M. Mori, *J. Org. Chem.* **2005**, *70*, 8605–8608.

[44] a) A. Ezoe, M. Kimura, T. Inoue, M. Mori, Y. Tamaru, *Angew. Chem.* **2002**, *114*, 2908–2910; *Angew. Chem. Int. Ed.* **2002**, *41*, 2784–2786; b) Y. Sato, T. Takanashi, M. Mori, *Organometallics* **1999**, *18*, 4891–4893; c) N. Saito, T. Yamazaki, Y. Sato, *Tetrahedron Lett.* **2008**, *49*, 5073–5076; d) H. Y. Cho, J. P. Morken, *J. Am. Chem. Soc.* **2010**, *132*, 7576–7577; e) N. Saito, A. Kobayashi, Y. Sato, *Angew. Chem.* **2012**, *124*, 1254–1257; *Angew. Chem. Int. Ed.* **2012**, *51*, 1228–1231.

[45] W. L. F. Armarego, C. L. L. Chai in *Purification of Laboratory Chemicals*, 5th ed., Butterworth–Heinemann, Amsterdam, **2003**.

[46] a) G. R. Fulmer, A. J. M. Miller, N. H. Sherden, H. E. Gottlieb, A. Nudelman, B. M. Stoltz, J. E. Bercaw, K. I. Goldberg, *Organometallics* **2010**, *29*, 2176–2179; b) H. E. Gottlieb, V. Kotlyar, A. Nudelman, *J. Org. Chem.* **1997**, *62*, 7512–7515.

[47] a) A. Bashall, A. D. Bond, E. L. Doyle, F. García, S. J. Kidd, G. T. Lawson, M. C. Parry, M. McPartlin, A. D. Wood, D. S. Wright, *Chem. Eur. J.* **2002**, *8*, 3377–3385; b) A. Bashall, E. L. Doyle, C. Tubb, S. J. Kidd, M. McPartlin, A. D. Woods, D. S. Wright, *Chem. Commun.* **2001**, 2542–2543.

[48] F. Dodds, F. García, R. A. Kowenicki, S. P. Parsons, M. McPartlin, D. S. Wright, *Dalton Trans.* **2006**, 4235–4243.

[49] A. R. Davies, A. T. Dronsfield, R. N. Haszeldine, D. R. Taylor, *J. Chem. Soc. Perkin Trans. 1* **1973**, 379–385; we found, that GP 1 constitutes an alternative route to **3**·Cl_2 and related diaryldichlorocyclophosphazanes.

[50] N. Burford, T. S. Cameron, K. D. Conroy, B. Ellis, C. L. B. Macdonald, R. Ovans, A. D. Phillips, P. J. Ragogna, D. Walsh, *Can. J. Chem.* **2002**, *80*, 1404–1409.

[51] a) M. Klussmann, L. Ratjen, S. Hoffmann, V. Wakchaure, R. Goddard, B. List, *Synlett* **2010**, 2189–2192; b) R. Zimmer, L. Schefzig, A. Peritz, V. Dekaris, H.-U. Reissig, *Synthesis* **2004**, 1439–1445.

[52] C.-S. Da, J.-R. Wang, X.-G. Yin, X.-Y. Fan, Y. Liu, S.-L. Yu, *Org. Lett.* **2009**, *11*, 5578–5581.

[53] C. Jonasson, A. Horvath, J. E. Bäckvall, *J. Am. Chem. Soc.* **2000**, *122*, 9600–9609.

[54] SAINT, Bruker AXS, Karlsruhe **1997–2008**.

[55] CrysAlisPro, Agilent Technologies UK Ltd., Oxford **2011**.

[56] *HKL* in Z. Otwinowski, W. Minor, *Methods Enzymol.* **1997**, *276*, 307.

[57] R. C. Clark, J. S. Reid, *Acta Crystallogr. Sect. A* **1995**, *51*, 887.

[58] R. H. Blessing, *Acta Crystallogr. Sect. A* **1995**, *51*, 33.

[59] SADABS, G. M. Sheldrick, Bruker AXS, Karlsruhe **2004–2008**.

[60] SCALE3 ABSPACK, CrysAlisPro, Agilent Technologies UK Ltd., Oxford **2011**.

[61] a) SUPERFLIP, L. Palatinus, EPF Lausanne (Switzerland), **2007**; b) L. Palatinus, G. Chapuis, *J. Appl. Crystallogr.* **2007**, *40*, 786.

[62] a) DIRDIF-2008, P. T. Beurskens, G. Beurskens, R. de Gelder, J. M. M. Smits, S. Garcia-Granda, R. O. Gould, Radboud University Nijmegen (The Netherlands), **2008**; b) P. T. Beurskens in *Crystallographic Computing 3* (Eds.: G. M. Sheldrick, C. Krüger, R. Goddard), Clarendon Press, Oxford, **1985**, p. 216.

[63] a) SHELXD, G. M. Sheldrick, University of Göttingen and Bruker Nonius, **2004**; b) G. M. Sheldrick, H. A. Hauptman, C. M. Weeks, R. Miller, I. Usón, *Ab Initio Phasing in International Tables for Crystallography, Vol. F* (Eds.: M. G. Rossmann, E. Arnold), IUCr and Kluwer Academic Publishers, Dordrecht, **2001**, pp. 333–351.

[64] a) SIR2004, M. C. Burla, R. Caliandro, M. Camalli, B. Carrozzini, G. L. Cascarano, L. De Caro, C. Giacovazzo, G. Polidori, R. Spagna,

CNR IC, Bari (Italy), **2004**; b) M. C. Burla, R. Caliandro, M. Camalli, B. Carrozzini, G. L. Cascarano, L. De Caro, C. Giacovazzo, G. Polidori, R. Spagna, *J. Appl. Crystallogr.* **2005**, *38*, 381.

[65] SHELXS-97, G. M. Sheldrick, University of Göttingen (Germany), **1997**.

[66] G. M. Sheldrick, *Acta Crystallogr. Sect. A* **2008**, *64*, 112.

[67] a) SIR92, A. Altomare, G. Cascarano, C. Giacovazzo, A. Guagliardi, M. C. Burla, G. Polidori, M. Camalli, CNR IC, Bari (Italy), **1992**; b) SIR92: A. Altomare, G. Cascarano, C. Giacovazzo, A. Guagliardi, M. C. Burla, G. Polidori, M. Camalli, *J. Appl. Crystallogr.* **1994**, *27*, 435.

[68] a) SHELXL-97, G. M. Sheldrick, University of Göttingen (Germany), **1997**; b) SHELXL-2013, G. M. Sheldrick, University of Göttingen (Germany), **2013**.

[69] P. v. d. Sluis, A. L. Spek, *Acta Crystallogr. Sect. A* **1990**, *46*, 194.

[70] a) PLATON, A. L. Spek, Utrecht University (The Netherlands); b) A. L. Spek, *J. Appl. Crystallogr.* **2003**, *36*, 7.

Received: June 18, 2013
Published online: August 28, 2013

